Received 1 October 2020; accepted 7 October 2020. Date of publication 16 October 2020;
date of current version 8 December 2020. The review of this article was arranged by Editor Sumei Sun.

*Digital Object Identifier 10.1109/OJVT.2020.3031656*

# Rate-Splitting Multiple Access: Unifying NOMA and SDMA in MISO VLC Channels

**SHIMAA NASER [1], PASCHALIS C. SOFOTASIOS [1,2] (Senior Member, IEEE), LINA BARIAH [1] (Member, IEEE), WAEL JAAFAR [3] (Senior Member, IEEE), SAMI MUHAIDAT [1,3] (Senior Member, IEEE), MAHMOUD AL-QUTAYRI [4] (Senior Member, IEEE), AND OCTAVIA A. DOBRE [5] (Fellow, IEEE)**

*(Invited Paper)*

[1] Center for Cyber-Physical Systems, Department of Electrical Engineering and Computer Science, Khalifa University, Abu Dhabi 127788, UAE
[2] Department of Electrical Engineering, Tampere University, 33014 Tampere, Finland
[3] Department of Systems and Computer Engineering, Carleton University, Ottawa, ON K1S 5B6, Canada
[4] Systems-on-Chip (SoC) Center, Department of Electrical Engineering and Computer Science, Khalifa University, Abu Dhabi 127788, UAE
[5] Faculty of Engineering and Applied Science University, Memorial University, St. John's, NL A1C 5S7, Canada

CORRESPONDING AUTHOR: PASCHALIS C. SOFOTASIOS (e-mail: p.sofotasios@ieee.org)

This work was supported by Khalifa University under Grant KU/FSU-8474000122 and Grant KU/RC1-C2PS-T2/8474000137. The work of Octavia A. Dobre was supported by the Natural Sciences and Engineering Research Council of Canada, through its Discovery program.

**ABSTRACT** The increased proliferation of connected devices requires a development of innovative technologies for the next generation of wireless systems. One of the key challenges, however, is the spectrum scarcity, owing to the unprecedented broadband penetration rate in recent years. Based on this, visible light communication (VLC) has recently emerged as an effective potential solution for enabling high-speed short-range communications. Yet, despite their undoubted advantageous features, VLC systems suffer from several limitations which constraint their capabilities. As a result, several multiple access (MA) techniques, such as space-division multiple access (SDMA) and non-orthogonal multiple access (NOMA), have been considered in VLC networks as an effective approach, among others, to circumvent these limitations. However, despite their achievable multiplexing gain, their overall performance is still limited compared to the overall potential of this technology. Motivated by this, the presented article offers two contributions: firstly, we provide an overview of the key MA technologies used in VLC systems and then we introduce rate-splitting multiple access (RSMA), and discuss its capabilities and potentials in VLC systems. Secondly, through realistic system modeling and simulations of an RSMA-based two-user scenario, we illustrate the flexibility of RSMA as well as its superiority in terms of the achievable weighted sum rate over NOMA and SDMA in the context of VLC. Finally, we discuss technical challenges, open issues, and research directions, along with the offered results and insights that are expected to be useful towards the effective practical realization of RSMA in VLC configurations.

**INDEX TERMS** Multiple-input multiple-output, non-orthogonal multiple access, rate-splitting multiple access, space-division multiple access, visible light communication.

## I. INTRODUCTION

The exponential growth of connected devices and emergence of the Internet-of-Everything (IoE), enabling ubiquitous connectivity among billions of people and machines, have been the major driving forces towards the evolution of wireless technologies. The aim of this is to ultimately support a plethora of new services, including enhanced mobile broadband and ultra-reliable and low-latency communications. Achieving this is rather vital since while the demand for new IoE services, e.g., extended reality, autonomous driving and tactile internet continues to grow, it is necessary for future wireless networks to operate with considerably high

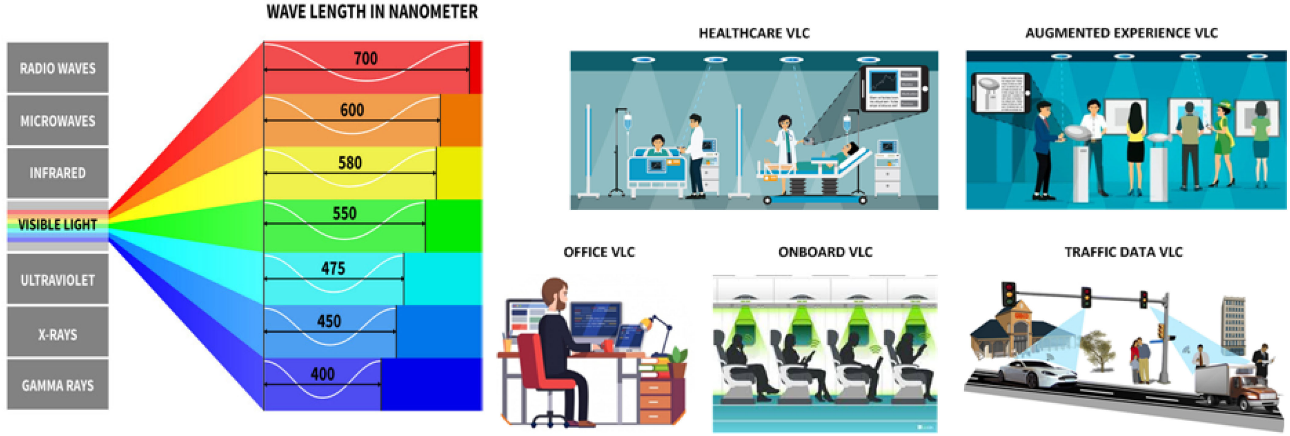


**FIGURE 1.** VLC spectrum and examples of its use.

reliability, low latency, and increased data rates. In this context, the notion of visible light communication (VLC) has emerged as a promising energy efficient and green wireless technology for massive connectivity of users with increased quality of service (QoS) requirements, such as high data rates.

In order to achieve effective realization of VLC, a simple and inexpensive modification is required to the existing lighting infrastructure [1]–[4]. It is recalled that the key attractive features of VLC include, but are not limited to, security, high degree of spatial reuse, and immunity to electromagnetic interference [5]. It is also noted that the advancement in solid-state electronics has introduced light emitting diodes (LEDs) as energy-efficient light sources, which are envisioned to constitute a core part of the next generation of wireless infrastructure. One of the interesting features of LEDs is their ability to rapidly switch between different light intensities in a way that is not perceptible to human eyes. This enables them to be the main technology for VLC systems. The key principle of VLC is to use emitted light from the LEDs to perform data transmission through intensity modulation and direct detection (IM/DD), without affecting the LEDs' main illumination function. The huge unregulated spectrum of visible light allows VLC to offload data traffic from radio-frequency (RF)/microwave systems while providing high data rates. VLC uses the 400 THz to 789 THz visible light spectrum, which is characterized by the features of low penetration through objects and secure communications as well as its capability to meet high QoS requirements. Moreover, due to the spatially-confined nature of the light being emitted from the LEDs, this technology is highly secure and efficient in the context of small optical attocells that are capable of enhancing the overall system capacity, without causing interference to co-existing RF-based systems [6]–[9]. Fig. 1 illustrates the VLC spectrum band along with indicative examples of its use in healthcare, work office, transportation, and smart cities. Also, the structure of the survey is depicted in Fig. 2. Table 1 shows acronynms and abbreviations used in this article.

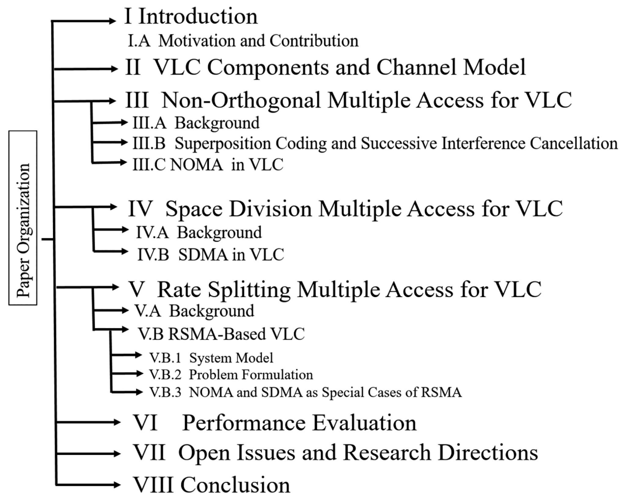


**FIGURE 2.** Organization of the paper.

### *A. MOTIVATION AND CONTRIBUTION*

Despite its advantages, VLC suffers from several drawbacks that limit its performance capabilities. For example, the limited modulation bandwidth and the peak optical power of LEDs are considered the main obstacles towards realizing the full potential of VLC systems [10]. Hence, extensive research efforts have been devoted in attempts to circumvent certain critical constraints, aiming to enhance the achievable spectral efficiency of VLC systems and networks. In particular, two research directions have been identified: in the first one, researchers focused on the design of dedicated VLC analog hardware and digital signal processing techniques. In the second one, researchers focused on enhancing the spectral efficiency through the development of different optical-based modulation and coding schemes, adaptive modulation, equalization, VLC cooperative communications, orthogonal and non-orthogonal multiple access (OMA/NOMA) schemes, and multiple-input multiple-output (MIMO) configuration [11].

The concept of optical attocells was recently introduced as an efficient method to enhance the overall system spectral

**TABLE 1.** List of Acronyms and Abbreviations

| Abbreviation | Definition | Abbreviation | Definition |
|---|---|---|---|
| ADT | Angle Diversity Transmitter | MU | Multi-User |
| AO | Alternating Optimization | MUD | Multi-User Detection |
| BD | Block Diagonalization | MUI | Multi-User Interference |
| BER | Bit Error Rate | NOMA | Non-Orthogonal Multiple Access |
| BC | Broadcast Channel | OCDMA | Optical Code-Division Multiple Access |
| CDMA | Code-Division Multiple Access | OFDM | Orthogonal Frequency-Division Multiplexing |
| C-NOMA | Code NOMA | OFDMA | Orthogonal Frequency-Division Multiple Access |
| CoMP | Coordinated multi-point | OMA | Orthogonal Multiple Access |
| CSI | Channel State Information | OOK | On-Off Keying |
| CSIT | CSI at Transmitter | P-NOMA | Power NOMA |
| DC | Direct Current | PD | Photo Detectors |
| DD | Direct Detection | QoS | Quality-of-Service |
| FoV | Field of View | RGB | Red, Green and Blue |
| ICI | Inter-Channel Interference | RSMA | Rate-splitting Multiple Access |
| IM | Intensity Modulation | SC | Super-position Coding |
| ISI | Inter-Symbol Interference | SDMA | Space Division Multiple Access |
| LED | Light Emitting Diode | SIC | Successive Interference Cancellation |
| LTE | Long-Term Evolution | SINR | Signal-to-Interference-Plus-Noise Ratio |
| LoS | Line-of-Sight | SNR | Signal-to-Noise Ratio |
| MA | Multiple Access | TDMA | Time-Division Multiple Access |
| MAC | Media Access Control | VLC | Visible Light Communication |
| MIMO | Multiple-Input Multiple-Output | WSMSE | Weighted Sum Mean Squared Error |
| MISO | Multiple-Input Single-Output | WSR | Weighted Sum Rate |
| MMSE | Minimum Mean-Square Error | ZF | Zero-Forcing |
| MSE | Mean-Square Error | ZF-DPC | Zero-Forcing Dirty-Paper |

efficiency and to overcome the limited coverage area of the LEDs. Typically, an LED array (assembly of LED chips arranged in a grid to serve as a single illuminating device) in each attocell operates as an access point that serves multiple users located in its coverage area. Since LED arrays utilized in indoor environments for the provision of uniform illumination have wide beams, it turns out that the respective illumination areas of adjacent cells overlap with each other. As a consequence, any user located in the overlapped area are subject to inter-cell interference, in addition to the inter-user interference caused by the messages of the nearby users within the same cell [12]. Hence, in order to improve the performance of the cell-edge users, various contributions have investigated the variation of time, frequency, or power allocation coordination schemes across the involved attocells [13]–[15]. For instance, multi-color schemes [16], multicarrier-based cell partitioning [17], optimized angle diversity receivers [18], and differential optical detection have been largely investigated in multi-cell VLC networks, showing an improvement on the achievable spectral efficiency compared to the single cell case [19]. However, the aforementioned techniques usually require dedicated receiver or transmitter architectures. For example, in large scale VLC networks, it is common that each attocell is composed of multi-luminaries that are connected through backhaul links. As a result, precoding schemes constitute effective methods for handling the incurred interference. To this end, different coordination techniques have been researched for precoding designs, also known as coordinated multi-point transmission techniques (CoMP). In CoMP transmission, the access points of different attocells are connected through backhual links in order to achieve an acceptable level of coordination/cooperation between them [20].

In the context of VLC, several optical OMA schemes have been proposed, including time-division multiple access (TDMA), orthogonal frequency-division multiple access (OFDMA) [21], and optical code-division multiple access (OCDMA) [22]. A main characteristic of these schemes rely on assigning orthogonal resources to different users. For example, in TDMA, different users are allocated different time slots for communication, while in OFDMA different users are assigned different orthogonal frequency sub-carriers. In OCDMA, users communicate at the same time and frequency, which can be achieved through the use of different orthogonal optical codes. In contrast, space-division multiple access (SDMA) exploits the spatial separation between users to provide full time and frequency resources. On the contrary, NOMA has been recently introduced as a spectrally-efficient multiple access (MA) scheme that allows different users to share the same time and frequency resources, leading to an enhanced spectral efficiency [23]. It is recalled that NOMA is realized either by assigning different power levels to different users (known as power domain (P)-NOMA) or by allocating different spreading sequences (called code domain (C)-NOMA). Also, resource allocation in NOMA is determined according to different criteria, such as link quality, users' fairness, targeted individual and sum rates, as well as users' QoS requirements.

In the same context, rate-splitting multiple access (RSMA) has recently emerged as a potentially robust and generalized MA scheme for future wireless systems, which is able to accommodate different users in a heterogeneous environment. In particular, research results have shown that RSMA in MIMO-based RF systems outperforms other common MA schemes, such as NOMA and SDMA, in terms of both spectral and energy efficiency [24]. The performance gain of RSMA comes from the fact that the transmitted signal of each user is divided into one or several common parts, and a private part. On the one hand, all common parts are multiplexed and encoded into a single (or several) common streams intended for all (or to a subset of) users. On the other hand, the private parts are encoded separately into multiple private streams, which are then superimposed with the common stream(s). The resulted super-symbol is then transmitted to all users over the VLC downlink channel. Then, at each user, the common streams are decoded first in order to obtain the common parts of the intended user, utilizing iterative successive interference cancellation (SIC). Subsequently, the private part is decoded while treating the other users' private parts as noise. It is noted here that NOMA scheme can be obtained from RSMA by treating some users' signals as common parts and the remaining as private parts. Likewise, SDMA can be realized from RSMA by using only the private parts to encode users' messages. Hence, this operation of splitting the messages into common and private parts enables RSMA to provide robust services for different network loads and users deployments.

It is recalled that MIMO channels in VLC systems are highly correlated in practice, which degrades the performance of linear precoding schemes. This has motivated the investigation of different receiver architectures and precoding schemes for mitigating the effect of channel correlation in MIMO VLC systems. Likewise, several contributions on the previously presented topics, namely OMA, NOMA and RSMA techniques, have been reported in the context of RF systems. Yet, only a small fraction of them have addressed their application in VLC networks, mainly for OMA and NOMA, and summarized these studies in surveys [25]–[27]. More importantly, none of them has discussed the integration of RSMA into VLC systems. Motivated by the above, in the present survey we shed light on several spectrally efficient MA schemes for VLC systems. Specifically, we present a comprehensive study of NOMA and SDMA schemes, with particular attention to MIMO-VLC systems. In addition, we address the potential integration of the RSMA scheme in MISO-VLC systems and quantify its achievable performance in comparison with that of the NOMA and SDMA counterparts. Finally, open issues and some interesting related research directions are discussed.

*Notation:* Bold upper-case letters denote matrices and bold lower-case letters denote vectors. $(\cdot)^T$ stands for the transpose operation, $\mathbb{E}(\cdot)$ denotes the statistical expectation, $|\cdot|$ is the absolute value operation, I is the identity matrix, $\mathbf{0}$ is the zero matrix, $\mathrm{tr}(\cdot)$ is the trace of a matrix, and $\mathcal{N}(0, \sigma^2)$ is a real-valued Gaussian distribution with zero mean and variance $\sigma^2$. Also, assuming a vector $\mathbf{z} = [z_1, \ldots, z_Z]$ with length $Z$, then $L_1(\mathbf{z}) = \sum_{i=1}^{Z} |z_i|$ denotes the $L_1$ norm.

## II. VLC COMPONENTS AND CHANNEL MODEL

In VLC, unlike RF systems, data is conveyed on the intensity of the emitted light from the installed LEDs; therefore, frequency and phase modulations cannot be applied. Moreover, due to the characteristics of intensity modulation, transmitted signals must be positive and real valued. Also, to ensure that the LED is functioning in its dynamic range, the transmitted peak power should not exceed a particular constant value. In this section, different components of VLC systems are presented in addition to VLC channel modeling.

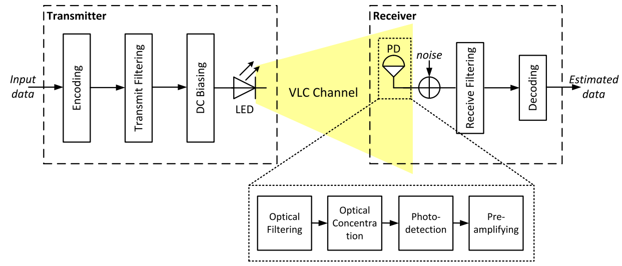


**FIGURE 3.** VLC transceiver components.

Fig. 3 illustrates the basic VLC transceiver components. At the transmitter, an illuminating device is utilized for data modulation through IM/DD. There are a variety of light sources that are available for optical communication, but the commonly used ones are LEDs and laser diodes. Particularly, LEDs are the most popular illuminating devices, due to their low fabrication cost. They are composed of solid-state semiconductor devices that produce spontaneous optical radiation when subjected to a voltage bias across the P-N junction [28]. The direct current (DC) bias excites the electrons resulting in released energy in the form of photons. In most buildings, white LEDs are preferred since objects seen under white LEDs exhibit similar colors to when they are seen under natural light. Two common designs are considered for white LEDs: in the first design, a blue LED with a yellow phosphor layer is utilized, while in the second design, red, green, and blue (RGB) LEDs are combined together. The first method is more popular, due to its simplicity and low implementation cost. However, it suffers from limited modulation bandwidth, due to the intrinsic properties of the phosphor coating. On the other hand, RGB LEDs are more suitable for color shift keying modulation, enabling higher achievable data rates [29].

It is recalled that VLC receivers comprise photo detectors (PDs), also known as non-imaging receivers or imaging (camera) sensors. These are used to convert incident light power into electrical current proportional to light intensity. A typical VLC receiver consists of an optical filter, optical concentrator, PDs, and pre-amplifier. The optical filter eliminates interference from ambient light sources, while the optical concentrator enlarges the effective reception area of the PD without increasing its physical size. The optical concentrator is characterized by three parameters, i.e., field of view (FoV), refractive index, and radius. In order to increase the achievable diversity gain of an optical communication link, multiple receiving units can be deployed with different orientations, optical filters, and concentrators. However, such deployment comes at the expense of additional receiver size and complexity. To address this issue, an imaging sensor with a single wide FoV concentrator can be used to create multiple images of the received signals. Imaging sensors consist of an array of PDs that are integrated with the same circuit. Yet, it is worth noting that the large number of PDs required for capturing high resolution photos renders them energy inefficient. Furthermore, the area of PDs in a VLC system is much

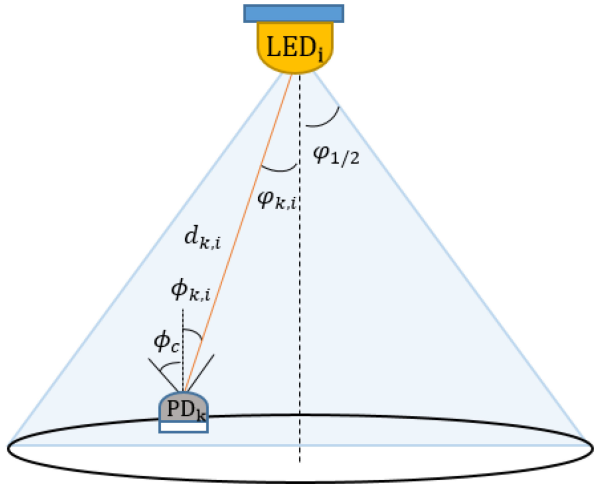


**FIGURE 4.** VLC channel model (link between LED *i* and PD *k*).

larger than the corresponding wavelength. Consequently, multipath fading in an indoor VLC environment does not occur [30], [31]. Nevertheless, indoor optical links suffer from dispersion, modeled as linear baseband impulse response. Also, the indoor optical wireless channels can be assumed quasi-static, due to the relatively low mobility of users and connected objects in indoor environments.

Typically, the channel of a VLC link can be modeled as follows: With the non-line-of-sight components neglected in the presence of stronger line-of-sight (LoS) ones, the DC channel gain from the $i^{th}$ LED to the $k^{th}$ PD can be expressed as [1]

$$h_{k,i} = \begin{cases} \frac{A_k}{d_{k,i}^2} R_o(\varphi_{k,i}) T_s(\phi_{k,i}) g(\phi_{k,i}) \cos(\phi_{k,i}), & 0 \leqslant \phi_{k,i} \leqslant \phi_c \\ 0, & \text{otherwise}, \end{cases} \tag{1}$$

where $A_k$ denotes the PD area, $d_{k,i}$ is the distance between the $i^{th}$ LED and $k^{th}$ PD, $\varphi_{k,i}$ is the transmission angle from the $i^{th}$ LED to the $k^{th}$ PD, $\phi_{k,i}$ denotes the incident angle with respect to the receiver, and $\phi_c$ is the FoV of the PD. These angles are illustrated in Fig. 4. Moreover, $T_s(\phi_{k,i})$ is the gain of the optical filter, and $g(\phi_{k,i})$ is the gain of the optical concentrator, expressed as

$$g(\phi_{k,i}) = \begin{cases} \frac{n^2}{\sin^2(\phi_c)}, & 0 \leqslant \phi_{k,i} \leqslant \phi_c \\ 0, & \phi_{k,i} > \phi_c. \end{cases} \tag{2}$$

In the above, $n$ is the refractive index and $R_o(\varphi_{k,i})$ is the Lambertian radiant intensity, which is given by

$$R_o(\varphi_{k,i}) = \frac{m+1}{2\pi} \left(\cos(\varphi_{k,i})\right)^m \tag{3}$$

with $m$ denoting the order of the Lambertian emission, namely

$$m = \frac{-\ln(2)}{\ln\left(\cos(\varphi_{1/2})\right)} \tag{4}$$

where $\varphi_{1/2}$ is the LED semi-angle at half power. For a typical VLC link, the received noise at the $k^{th}$ PD can be modeled as a Gaussian random variable with zero mean and variance

$$\sigma_k^2 = \sigma_{k,sh}^2 + \sigma_{k,th}^2 \tag{5}$$

where $\sigma_{k,sh}^2$ and $\sigma_{k,th}^2$ are the variances of the shot and thermal noises at the $k^{th}$ PD, respectively. The shot noise is caused by the high rate of the physical photo-electronic conversion process, whose variance can be written as

$$\sigma_{k,sh}^2 = 2qB\left(\zeta_k h_{k,i} x_i + I_{bg} I_2\right) \tag{6}$$

where $q$ represents the electronic charge, while $\zeta_k$ denotes the detector responsivity. Also, $x_i$ is the transmitted signal by the $i^{th}$ LED, $B$ is the corresponding bandwidth, $I_{bg}$ is the background current, and $I_2$ denotes the noise bandwidth factor. On the other hand, the thermal noise results from the transimpedance receiver circuitry and its variance at the $k^{th}$ PD is given by

$$\sigma_{k,th}^2 = \frac{8\pi K T_k}{G} \eta A_k I_2 B^2 + \frac{16\pi^2 K T_k \gamma}{g_m} \eta^2 A_k^2 I_3 B^3 \tag{7}$$

where $K$ is the Boltzmann's constant, $T_k$ is the absolute temperature, $G$ is the open-loop voltage gain, $A_k$ is the PD area, $\eta$ is the PD's fixed capacitance per unit area, $\gamma$ is the field-effect transistor (FET) channel noise factor, $g$ is the FET transconductance, and $I_3 = 0.0868$ [1]. Modern infrastructures are commonly equipped with LED fixtures or arrays. A single fixture is composed of $Q$ LEDs, and may be viewed as a single VLC source,[1] with the DC channel gain given by

$$h_{k,j} = \begin{cases} A_k \sum_{i=1}^{Q} d_{k,j,i}^{-2} R_o(\varphi_{k,j,i}) T_s(\phi_{k,j,i}) g(\phi_{k,j,i}) \cos(\phi_{k,j,i}), \\ \qquad 0 \le \phi_{k,j,i} \le \phi_c \\ 0, \ \text{otherwise} \end{cases} \tag{8}$$

where $d_{k,j,i}$ and $\varphi_{k,j,i}$ denote the respective distance and transmission angle between the $i^{th}$ LED in the $j^{th}$ fixture and the $k^{th}$ PD, whereas $\phi_{k,j,i}$ is the incident angle with respect to the receiver. Since the separation between LEDs in the same fixture is negligible compared to the distance between the fixture and the $k^{th}$ PD, then distances and angles implicating index $i$ can be assumed approximately the same for all LEDs. Hence, the channel gain from the $j^{th}$ fixture to the $k^{th}$ PD can be given by

$$h_{k,j} \approx \begin{cases} Q\ h_{k,i}, & 0 \le \phi_{k,j,i} \le \phi_c, \ \forall i \\ 0, & \text{otherwise}. \end{cases} \tag{9}$$

In the following sections, we provide an in-depth study of the common MA schemes in the context of VLC.

## III. NOMA FOR VLC

### A. BACKGROUND

Inspired by the promising multiplexing gain achieved by conventional MA techniques, which were initially developed for

[1] In the remainder of this paper, we interchangeably designate by LED a fixture of LEDs.

RF systems, optical MA methods have received a considerable attention in recent years. To this end, conventional OMA schemes such as OFDMA and TDMA have been extensively studied in the context of VLC, in which users are allocated orthogonal frequency/time resources. In the same context, several optical OFDM-based MA techniques were proposed, such as DC biased optical OFDM, asymmetrically clipped OFDM, asymmetrically clipped DC-biased optical OFDM, fast-OFDM and, polar-OFDM. However, it is recalled that OFDM suffers from the high peak-to-average power ratio, which is difficult to overcome in VLC systems due to the non-linearity of LEDs [21], [32]–[35]. It is also noted that OMA schemes efficiently mitigate interference among users' signals by allocating orthogonal resources. However, the number of served users in these scenarios is limited and cannot exceed the number of available orthogonal resources. This concern is also true in the case of VLC systems.

Motivated by the above, researchers have recently focused on the design of novel NOMA techniques as a promising candidate to enhance spectral efficiency in 5 G and beyond networks [23]. The key principle is to allow different users to share the same frequency resources simultaneously at the expense of multi-user interference (MUI). To perform multi-user detection (MUD), different users are assigned distinct power levels based on their channel gains, which is referred to as P-NOMA, or different spreading sequence, known as C-NOMA [23], [36], [37]. In RF systems, P-NOMA was considered as a candidate for the downlink communication of various standardization activities such as the 3rd generation partnership project (3GPP) standard LTE Release 13 [38]. Furthermore, P-NOMA has been envisioned as a key solution in 5G mobile systems [30]. On the contrary, both P-NOMA and C-NOMA have been considered for the uplink communication, in order to serve a larger number of users. In downlink P-NOMA systems, superposition coding (SC) at the base station and SIC at the receiver are utilized to transmit and detect the intended user's signal by eliminating users' signals with higher power levels, respectively. Yet, in the uplink P-NOMA systems, the transmitted power is limited by the end users, where for each individual user the transmitted power should be carefully adjusted such that the user with better channel gain has more power contribution in the received signal. At the base station, the message of the user with the best channel gain is decoded first. Then, a subsequent SIC is performed in order to decode the messages of the weaker users, which is the opposite of the downlink P-NOMA scheme [30], [38].

In C-NOMA, users are multiplexed in the code domain, in which each user is assigned a different code. Unlike the conventional code-division multiple access (CDMA), where dense spreading sequences are used, C-NOMA utilizes non-orthogonal sequences with low cross correlation or sparse spreading sequences to efficiently reduce inter-user interference [39]–[42], and hence, enhance the overall system performance. Specifically, optimal performance can be achieved in C-NOMA-based VLC systems by exploiting optical code sequences [43]. At the receiver, multi-user detection can then be realized by adopting message passing algorithms. It is noted that different versions of C-NOMA have been developed, such as low-density spreading (LDS)-CDMA [44], low-density spreading (LDS)-OFDM [45], and sparse code multiple access (SCMA) [46]. LDS-CDMA utilizes low density spreading sequences in order to reduce the interference on each chip compared to the traditional CDMA. On the other hand, LDS-OFDM can be thought as a combination of both OFDM and LDS-CDMA, where the resulted chips from the implementation of LDS-CDMA are transmitted over a set of sub-carriers. Finally, SCMA is a form of LDS-CDMA, where the information bits can be directly mapped to a distinct sparse codeword. Yet, although C-NOMA has a potential to enhance spectral efficiency, it requires additional bandwidth, challenging codebook design, and is not easily applicable to the current systems compared to P-NOMA, which has a simple implementation in the existing networks. For theses reasons, most of the research on NOMA systems have extensively considered the performance of P-NOMA [30], [47], [48]. In VLC systems, the research on C-NOMA is limited only to [42]. Therefore, this scheme requires further investigation in the context of VLC. It is also worth noting that uplink VLC scenarios are impractical due to the power limitations of portable devices and the unpleasant radiance produced by end users. So, it is expected that the current VLC technologies will rely on RF or infrared communications for the uplink wireless transmissions [49]–[51]. Consequently, most of the research efforts on NOMA in VLC systems have focused on the downlink scenario. A basic system model for two-user downlink P-NOMA in VLC systems is illustrated in Fig. 5.

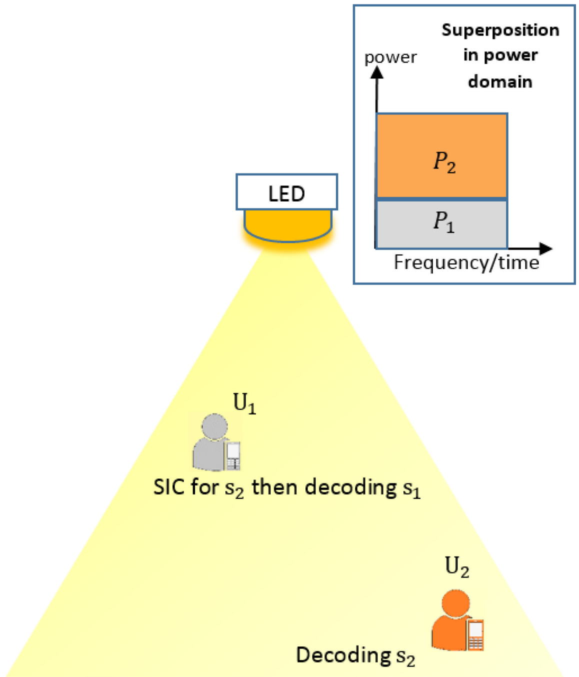


**FIGURE 5.** Scenario of two users P-NOMA in VLC.

For indoor VLC systems, P-NOMA is preferred for several reasons [52]. First, P-NOMA depends on the channel state information (CSI), which can be readily available in VLC systems. Second, P-NOMA achieves the best performance in high SNR regimes, which is a common SNR regime in VLC channels [3]. Third, P-NOMA performs best when the channels of the involved users are distinct. In VLC systems, the underlying symmetry issue of the channels has been addressed in [53], where the authors proposed reducing channels' symmetry by an adaptive tuning of the semi-angle of the LEDs and the receiver's FoV, as well as in [54], where advance receiver structures were considered. Finally, P-NOMA can be easily integrated with various technologies, such as MIMO and cooperative networks [46]. All these reasons motivated an extensive focus on investigating P-NOMA-based VLC systems.

### B. SUPERPOSITION CODING AND SUCCESSIVE INTERFERENCE CANCELLATION

The SC was first introduced in 1972 by Cover [55] as a method to transmit different signals to several receivers through a single source. In order to make SC practical in a two-user scenario, the transmitter encodes the data of the two users as a two-layer single signal. Then, one receiver recovers the messages of the two layers, while the other recovers only one message from one-layer and ignores the message of the second layer. The SC in NOMA is realized by allocating a distinct power level to each user. In particular, users with weak channel conditions are allocated high power coefficients. On the contrary, users with strong channel gains are assigned low power coefficients [38]. For instance, in Fig. 5, the second user $U_2$ is allocated a fraction $P_2$ of the total power, and the first user $U_1$ is allocated $P_1$, such that $P_1 < P_2$. Based on this, since the weaker user $U_2$ is allocated higher power, it can directly decode its signal while treating the signal of the other user as noise. On the contrary, user $U_1$ has to remove the interference by decoding $U_2$ signal with the aid of SIC, before detecting its own signal.

### C. NOMA IN VLC

Several studies have considered the performance of different NOMA configurations in VLC systems. In [41], the symbol error rate (SER) of C-NOMA-based VLC system was investigated, where users exhibited identical error rate performance at different locations. On the other hand, recently published papers showed that P-NOMA is a rather efficient MA scheme in VLC systems, due to the aforementioned reasons [53], [56], [57]. Furthermore, reported results showed that NOMA[2] outperforms OMA techniques, such as OFDMA and TDMA, in terms of system capacity and number of simultaneously served users, particularly in single-input single-output broadcast channels and for certain channel strength disparities among users [58]–[61]. The work in [62] considered the performance of NOMA VLC system when users have random vertical orientations. In particular, the authors proposed users scheduling techniques and feedback mechanisms to boost the spectral efficiency. Moreover, a hybrid NOMA-OFDM system was investigated and shown to exhibit superior performance in terms of the achievable rate over OMA-OFDM systems [63], [64]. Likewise, for uplink NOMA-based VLC communications, joint detection was proposed in [65] to decode the messages of multiple users.

It is noted here that although NOMA is efficient for scenarios where the number of users is higher than the number of available orthogonal resources, its complexity grows proportionally and rapidly to the number of users. This is because the $k^{th}$ user is required to decode the messages of the $k-1$ users before detecting its own signal. A relatively simple approach to address this issue is to group the users into small clusters, such that users of the same cluster communicate based on NOMA, whereas the different clusters are scheduled with the aid of an OMA technique. In particular, MIMO technology can be leveraged to provide additional gains for transmissions, which can be realized through precoded SC and hybrid SDMA-NOMA or OMA. In precoded SC, all users are sorted based on their effective precoded channel gains in a single cluster [66]–[68]. On the contrary, in hybrid SDMA/NOMA, users are grouped in clusters separated by SDMA.[3] [69], where the users of a single cluster are served using NOMA. It was demonstrated in [69] and [70] that MIMO-NOMA outperforms MIMO-OMA in terms of sum rate and user fairness. However, despite the aforementioned advantages of MIMO-NOMA systems, they come at the expense of a complex transmitter design, where joint optimization of the precoding/decoding orders of the signals is required for different users.

As explained earlier, MIMO designs can be realized by assuming multiple transmitting LEDs and multiple PDs at the receiver. Such a system cannot employ the same power allocation methods designed for single transmitting LED NOMA VLC systems, such as gain ratio power allocation (GRPA) [31]. Accordingly, several power allocation strategies have been proposed in the literature for MIMO-NOMA RF systems, e.g., hybrid precoding and post-detection [71], and signal alignment [72], [73]. However, their counterpart in the MIMO-NOMA VLC is almost non-existent. To the best of the authors' nowledge, only Chen *et al.* investigated NOMA-based MIMO VLC systems and proposed a power allocation strategy, called normalized gain difference power allocation (NGDPA) [74]. The reported results for NGDPA illustrated a sum rate improvement of 29.1% compared to GRPA.

Multi-cell NOMA in the context of VLC is also a topic that has not been sufficiently investigated in the open technical literature. In [75], Zhang *et al.* proposed a user grouping scheme based on users' locations aiming to minimize the interference caused by multi-cell deployment. Further, the authors in [76] proposed a joint NOMA transmission scheme to serve users in overlapping regions of different cells. In [77], Shi *et al.*

[2]In the remainder of the paper, P-NOMA is designated by NOMA.

[3]SDMA is discussed in detail in Section IV

investigated the use of offset quadrature amplitude modulation (OQAM)/OFDM-NOMA scheme in a multi-cell VLC system. Although NOMA schemes outperform OMA-based VLC systems in terms of spectral efficiency, the multiplexing gain of NOMA is highly affected by channel symmetry. In the context of VLC, channel symmetry is a major challenge as the communication is usually considered due to the LoS components [49], [52]. Indeed for small cell design, where the number of users is considered relatively large, it is inefficient to multiplex all users using NOMA, as this may lead to an increased complexity and unsuccessful SIC operation. Therefore, hybrid NOMA/OMA schemes are promising solutions to realize a trade-off between multiplexing gain, computational complexity, and error propagation. In hybrid NOMA/OMA systems, users are split into multiple groups, where users within the same group employ NOMA, while different groups are multiplexed using OMA. User pairing and grouping represents a key challenge in hybrid NOMA/OMA systems that requires sophisticated algorithms to exploit the full potentials of NOMA. However in VLC systems, as users mobility is relatively low, the variation in the channel conditions is relatively small, hence, user pairing and grouping requires less complicated algorithms compared to RF systems.

The effect of user pairing and grouping has been extensively studied in RF systems [78]–[82], but, its application in VLC systems requires further investigations. For instance, in [59], [83], the authors adopted channel gain-based pairing strategy that aims to maximize the system's throughput. This strategy relies on selecting two users with the most distinctive channel gains to perform NOMA. However, their approach causes interference to users with correlated channels. In [84], the authors proposed individual and group-based NOMA users pairing in a VLC system and showed that a near-optimal sum-rate performance can be achieved. Moreover, user grouping based on users' locations was proposed in [75] in order to reduce the interference in multi-cell VLC networks, where users in each group are served by only one access point using NOMA. On the other hand, the authors in [85] proposed a hybrid OMA/NOMA scheme for attocellular VLC based on a smart transmitter that can select dynamically the adequate MA technique according to the environment conditions. Finally, the authors in [86] proposed an efficient user pairing for the cases of having odd and even number of users. First, users are ordered in ascending order based on the channel strength; then, they are either grouped into two or three groups depending on whether the number of the users is even or odd. Then pairing is performed by choosing one user from each group starting from the users with the lowest channel gain. Reducing channels' correlation for the end users is another method for enhancing the performance of NOMA system. In [53], the authors proposed an adaptive adjustment of the semi-angle of the LEDs and the FoV of the PD in order to create dissimilar channels. Additionally, the use of different advanced receiver architectures that are capable of reducing the correlation of the involved channels is a potential solution that calls for further investigation [54]. Nevertheless, the enhancement of NOMA performance through reducing channels symmetry need to be further explored in the context of VLC. Finally, it is noted that NOMA-based hybrid VLC/RF systems have been proposed as acceptable solutions that are capable of compensating for the limitation of VLC systems, particularly in uplink communication scenarios [87]–[89]. In the same context, hybrid wavelength division multiplexing (WDM)-NOMA has been proposed in [90], where multi-color LEDs are used to allow simultaneous transmissions at different wavelengths. The most relevant existing contributions on NOMA in VLC systems is summarized in Table 2.

## IV. SDMA FOR VLC

### A. BACKGROUND

In recent building designs, it is common to have multiple illuminating LEDs in indoor spaces. In this context, channel access in VLC systems can be realized either through multiple access channel (MAC) or broadcast channel (BC). To this end, most research efforts have focused on the analysis of downlink BC of MU-MIMO, with an emphasis on the data rate performance. Such systems experience interference when orthogonal frequency/time resources are limited. MUI is a common issue in MU-MIMO systems, which can be eliminated at the receiver using an efficient MUD technique [91], [92]. However, the implementation of MUD in VLC systems suffers from high complexity and energy inefficiency. Therefore, SDMA, which is based on data precoding at the transmitter, constitutes a promising alternative solution.

### B. SDMA IN VLC

An early implementation of SDMA is based on block diagonalization (BD), which is a generalized form of channel inversion precoding [93]. Although BD is a simple linear precoding technique, its application is limited to the scenario where the number of transmitting LEDs is larger than the total number of served users, i.e., overloaded regime. The authors in [94] used BD precoding in downlink MU-MIMO VLC and showed that BD is constrained by the correlation of the involved wireless links. Hence, a scheme that reduces this correlation was proposed, based on the adjustment of PDs' FoVs. Yu *et al.* developed in [95] linear zero-forcing (ZF) and ZF dirty paper coding (ZF-DPC) schemes in order to eliminate MUI and maximize the throughput or max-min fairness. However, in [96], the authors relaxed the ZF condition by applying the minimum mean squared error (MMSE) as a performance metric for the precoder design, in both perfect and imperfect CSI scenarios. In [97], an optimal mean squared error (MSE) precoder was designed in order to minimize the BER, under per-LED power constraints. The transceiver design was later simplified by adopting a ZF precoder. The corresponding results showed that the simplified scheme outperforms the conventional ZF precoder in terms of BER, while MSE achieves the best performance. Similar designs were proposed in [98], where an optimal ZF precoder was obtained using an iterative concave-convex procedure, aiming at maximizing

**TABLE 2.** VLC Related Work on NOMA

| Reference | System Model | Objective | Findings |
|---|---|---|---|
| [41] | Single-cell downlink C-NOMA | Analysis and evaluation of the SER | Using adequate power allocation, users at different locations achieve almost an identical SER |
| [53] | Single-cell downlink NOMA | Derivation of closed-form expression for the bit error rate (BER) | Closed-form expressions match simulation results |
| [59] | Single-cell downlink NOMA | Derivation of closed-form expressions for the coverage probability and ergodic sum rate | NOMA outperforms conventional OMA scheme |
| [62] | Single-cell downlink NOMA | Derivation of closed-form expressions for the sum rate and outage probability | Analytical results agree with simulation results and near-optimal sum rate is achieved using a limited feedback scheme |
| [63], [64] | Single-cell downlink NOMA-OFDM | Maximization of the sum rate | NOMA-OFDM is superior to OMA-OFDM system, in terms of achievable data rate |
| [65] | Single-cell uplink NOMA | Evaluation of BER based on phase pre-distorted joint detection | Improved BER performance compared to NOMA based on SIC for different power values |
| [74] | MIMO-NOMA | Maximization of the sum rate | NGDPA improves the sum rate performance compared to GRPA |
| [75] | Downlink MU-multi-cell NOMA | Maximization of the sum rate and max-min rate criterion | User grouping and power allocation optimized, hence achieving higher sum user rate than OMA |
| [76] | Downlink MU-multi-cell NOMA | Maximization of the sum rate | Joint transmission (JT) NOMA achieves higher sum rates compared to the frequency reuse factor-2 NOMA |
| [77] | Downlink MU-multi-cell OQAM/OFDM-NOMA | Evaluation of spectral efficiency, BER, and error vector magnitude | Proposed scheme outperforms OFDM-NOMA and is more robust to inter-cell interference |
| [85] | Multi-cell hybrid OMA/NOMA | Evaluation of sum rate, outage probability, and fairness performances | Dynamically selecting the adequate MA technique achieves better performances that static configuration |
| [87], [88] | Downlink hybrid VLC/RF | Maximization of the sum rate | Optimal joint user grouping and power allocation based on game theory was proposed; this outperforms the standard opportunistic scheme |
| [89] | Cooperative NOMA VLC/RF with simultaneous wireless information and power transfer (SWIPT) | Derivation of closed-form expression for the outage probability | A trade-off on rate splitting allows outage performance balancing among users |
| [90] | Hybrid WDM-NOMA | Maximization of the sum rate | WDM-NOMA outperforms NOMA in terms of sum rate |

the achievable per-user data rate. Then, the authors simplified the precoder design using the high signal-to-noise ratio (SNR) approximation. In [99], Shen *et al.* proposed a different beamforming technique aiming at maximizing the sum rate of a virtual MIMO VLC system. Beamforming was designed using the sequential parametric convex approximation method, and it has been shown through simulations that it outperforms conventional ZF-based beamforming, particularly for highly correlated VLC channels and low optical transmit power. Likewise, Marshoud *et al.* developed in [100] an optical adaptive precoding for downlink MIMO VLC systems, under perfect and imperfect CSI. The corresponding BER results showed that the proposed scheme is more robust to imperfect CSI and channel correlation than conventional channel inversion precoding. In the same context, the authors of [101] investigated different precoding techniques for an OFDM-based MU-MIMO VLC system, where precoding is applied at each sub-carrier using either ZF or MMSE techniques. The reported results demonstrated that MMSE precoding outperforms ZF precoding in terms of the achievable spectral efficiency for the case of low SNR and correlated VLC channels. In [102], the sum rate maximization problem was reformulated as a weighted MMSE (WMMSE) problem to jointly design the precoding and receive filter coefficients. A similar approach was also considered in [103]. Finally, Adasme *et al.* proposed in [104] a hybrid approach, called spatial TDMA (STDMA), where full connectivity is achieved by allowing simultaneous data transmission of multiple nodes within an optimized schedule.

The contribution in [105], [106] focused on precoding designs for coordinated multi-point (CoMP) MU-MIMO VLC systems. Through numerical analysis, the authors showed improvements in terms of signal-to-interference-plus-noise ratio (SINR) and weighted sum MSE (WSMSE), respectively. Additionally, Yin *et al.* considered in [107], [108] different SDMA grouping algorithms to obtain a trade-off between the Jain's fairness index and area spectral efficiency for a CoMP-VLC system through the utilization of linear ZF precoding. The authors in [12] proposed a joint precoder and equalizer design based on interference alignment for MU multi-cell MIMO VLC systems under imperfect CSI, whereas in [20], different levels of coordination/cooperation were considered using a ZF precoder.

It is worth noting that SDMA can be also realized using an angle diversity transmitter (ADT), which consists of multiple directional narrow-beam LED elements. An ADT creates independent narrow-band beams towards spatially deployed users, while achieving the same coverage as a single wide-beam transmitter [109]–[111]. ADTs can also replace conventional single-element transmitters in multi-cell scenarios such that more power is directed towards each user, which in turn improves the communication's reliability [112]. In order to avoid interference among users, spatial separation needs to be implemented by adequately allocating transmit power

**TABLE 3. VLC Related Work on SDMA**

| Reference | System Model | Objective | Findings |
|---|---|---|---|
| [93], [94] | MU-MISO with BD precoding | Evaluation of the BER | With enough transmit power, a data rate of 100 Mbps is achieved for BER=$10^{-6}$ |
| [95] | MU-MISO with ZF or ZF-DPC precoding | Maximization of the throughput and max-min fairness | ZF-DPC outperforms linear ZF, in particular when users are close to each other |
| [96] | MU-MISO with MMSE precoding | Evaluation of the optimal linear MMSE precoder under perfect and imperfect CSIT | Linear MMSE precoding is able to separate the broadcast signals at the VLC receivers |
| [97] | MU-MISO with MMSE/ZF precoding | Minimization of the MSE and evaluation of the BER | MMSE precoding achieves beast results, while proposed simplified ZF approaches MMSE performance for a small number of (or dispersed) users |
| [98] | MU-MISO with ZF precoding | Maximization of the sum rate and max-min fairness | The generalized-inverse ZF design achieves better performance than the pseudo-inverse ZF design, in particular for high SNRs |
| [99] | MU-MISO with ZF precoding | Maximization of the sum rate | The proposed approach does not restrict the co-channel interference to zero, and thus, achieves a higher sum rate than conventional ZF techniques |
| [100] | MU-MISO with adaptive precoding | Derivation of closed-form expression and evaluation of BER under perfect and imperfect CSIT | Adaptive precoding provides performance enhancement compared to conventional channel inversion precoding |
| [101] | MU-MIMO OFDM with ZF/MMSE precoding | Evaluation of the spectral efficiency | Sub-carrier with higher index achieves a higher spectral efficiency, particularly for highly correlated users, and MMSE outperforms ZF for low transmit power and close users |
| [102] | MU-MISO with BD precoding | Maximization of the sum rate with imperfect CSIT | Robust precoding is designed using BD and WMMSE to suppress MUI and channel estimation errors |
| [103] | MU-MIMO with joint MMSE precoding and equalizing | Minimization of the MSE and evaluation of the BER in presence of CSIT errors | Proposed joint optimization method demonstrates BER improvements when experiencing imperfect CSIT |
| [104] | MU-STDMA | Minimization of the total scheduling time and power consumption | STDMA achieves full connectivity, and the proposed greedy algorithm reduces the processing time |
| [105], [106] | Multi-cell MU-MIMO CoMP with MMSE precoding | Minimization of the WSMSE | Proposed approach realizes low-complexity interference mitigation compared to CoMP JT |
| [107], [108] | CoMP SDMA with ZF precoding | Evaluation of the Jain's fairness index and of area spectral efficiency | The proposed grouping algorithm achieves better area spectral efficiency-fairness trade-off compared to existing benchmarks |
| [12] | Multi-cell MU-MIMO joint MMSE precoding and equalizing | Minimization of the MSE and sum rate evaluation with imperfect CSIT | The joint design of the precoder and equalizer efficiently reduces inter-user interference and inter-cell interference, and achieves better performance compared to existing MMSE and max-rate designs |
| [20] | Multi-cell MU-MIMO CoMP with ZF precoding | Maximization of the sum rate | Partial cooperative precoding and coordinated precoding outperform per-cell coordinated precoding when the number of users is not large compared to the number of the LEDs or for high transmit power |
| [110], [111] | SDMA using ADTs | Evaluation of the throughput | The use of ADTs improves the performance of multi-user systems, and optical SDMA outperforms optical TDMA in terms of throughput |
| [112] | Attocell SDMA downlink using ADT | Derivation of closed-form expression for the spectral efficiency | inter-cell interference is mitigated and optical SDMA outperforms optical TDMA |
| [114] | MU-MIMO using ADTs | Maximization of the minimum SINR and evaluation of the rate per-user with imprefect CSIT | The proposed precoding and receiver design is robust to channel estimation errors and achieves gains compared to non-robust receiver design |

to the beams. Subsequently, each receiver attempts to detect its signal by treating any interference as noise. Nevertheless, despite the potential of ADT for interference reduction, it requires a complex optical front-end to supply independent signals to multiple LED elements.

Notably, SDMA simplifies the transmitter and receiver designs, compared to NOMA. However, it becomes inefficient as soon as the number of users exceeds the number of transmit LEDs, i.e., the case of an overloaded scenario. It should be noted that the number of LEDs has to be more than or equal to the number of users in order to guarantee interference reduction. Moreover, since SDMA depends highly on the CSI at the transmitter (CSIT) in order to mitigate interference, its performance degrades with imperfect and/or outdated CSI [100], [113], [114]. Finally, due to the unique characteristics of IM/DD, which require signals to be real and unipolar, it is very difficult to pair orthogonal users together, as in RF systems. The accomplished work on SDMA in VLC is summarized in Table 3.

## V. RSMA FOR VLC

Although NOMA realizes simultaneous transmission of a large number of users in overloaded scenarios and SDMA achieves spatial separation between users in underloaded scenarios, their performance is highly dependent upon users' deployments, channel conditions, and availability of CSIT. Therefore, a generalized configuration, which can optimize the utilization of resources for both overloaded and underloaded scenarios whilst exhibiting increased robustness to CSIT estimation errors, is of paramount importance. This has been the main motivation underlying the proposal of RSMA as a generalized scheme, where NOMA and SDMA can be considered as special cases.

### A. BACKGROUND

The basic concept of rate-splitting was first introduced in [115] for a two user single-input single-output BC scenario. In [24], [116], RSMA was proposed as a powerful and generalized MA technique for RF systems. It was demonstrated that RSMA could potentially offer improvements as a MA technique, by allowing wireless networks to efficiently serve multiple users with different capabilities in overloaded and underloaded scenarios. According to the key principle of RSMA, which relies on the implementation of linearly precoded rate splitting at the transmitter and SIC at the receiver, it has been shown that this MA scheme is capable of bridging the gap between NOMA and SDMA techniques. Authors in [24] proposed a simplified version of the generalized RSMA scheme referred to as one-layer RSMA. In one-layer RSMA, users' messages are split into common and private parts at the transmitter. Then, a combiner is used to multiplex the common parts of all users and encode them into a single common stream. Meanwhile, the private parts are encoded separately into multiple private streams, whilst a linear precoder is subsequently used for mitigating the incurred MUI. Finally, all precoded streams are superimposed on the same signal and sent over a VLC BC channel. It is worth noting that one-layer RSMA simplifies both the scheduler and receiver design compared to the generalized RSMA scheme while still achieves a good performance compared to NOMA and SDMA. At each user, the common stream is decoded at first and the user's intended data is extracted. Then, interference introduced by the common stream is eliminated using SIC, as in NOMA. Subsequently, the private part of each user's message can be decoded, while treating the private parts of other users' messages as noise, as in SDMA. This mechanism is illustrated in (Fig. 1, [24]).

RSMA depends mainly on the splitting design of messages and power allocation strategies between common and private parts of users' messages. Hence, extensive research efforts have been devoted to the investigation of these issues in order to improve the efficiency of RSMA in the context of RF-based communications. To this effect, the authors in [24] provided an analytical framework to study the performance of RSMA in MU-MISO BC channels. The reported results proved that RSMA outperforms NOMA and SDMA in terms of sum rate for different users' setups. Dai *et al.* investigated in [117] RSMA with massive MIMO and imperfect CSIT. They proposed a hierarchical-rate-splitting (HRS) framework where two different types of common messages are defined, which can be decoded by either all users or by a subset of them. Then, the associated sum rate performance was investigated in order to adjust the precoders of common messages. Numerical results illustrated the superiority of HRS compared to conventional techniques such as TDMA and BC with user scheduling. This work was extended in [118] to a MU millimeter wave (mmWave) case, where CSIT is either statistical or quantized. Similar to [117], Joudeh *et al.* proposed in [119] a hybrid RSMA messages precoding in order to achieve max-min fairness amongst multiple co-channel multicast groups. The superiority of their approach is proved through degree-of-freedom analysis and simulation results. The authors in [120] evaluated the robustness of RSMA, in the presence of hardware impairments, such as phase distortion and thermal noises, and the availability of perfect/imperfect CSIT. In addition, Abdelhamid *et al.* investigated in [121] the use of channel inversion precoding for MU-MIMO RSMA system, where phase-shift-keying was the adopted modulation scheme. Results showed that RS combined with channel inversion has a sum rate improvement compared to RS with ZF or other MA schemes. Moreover, the authors in [122] incorporated RS with DPC to achieve the largest rate region for MISO BC with partial CSIT for different network loads and users' deployments. In [123], Hao *et al.* proposed a practical scheme for private symbols encoding in RSMA using the conventional ZF beamforming. Then, they studied the sum rate performance for a two-user BC channel with limited CSI feedback. In [124], the authors considered the trade-off between the spectral efficiency and energy efficiency for RSMA in multi-antenna BC channels. It was shown that RSMA achieves an improvement in terms of both spectral and energy efficiency. The use of RSMA in the downlink of a MISO SWIPT BC channel was investigated in [125], where the sum rate performance of rate-splitting was evaluated and compared with other MA schemes. A further study of RSMA in downlink CoMP JT networks was considered in [126], where results showed the superiority of RS in JT over SDMA- or NOMA-based JT. Also, in [127], Zhang *et al.* considered a cooperative rate splitting strategy based on the three-node relay channel, and demonstrated the enhanced performance of this scheme compared to cooperative-based NOMA scheme. Similar results were reported in [128], where the max-min fairness was used as a metric for a $K$-user MISO BC with user's relaying cooperative communication. The authors in [129] adopted a RS strategy to overcome the saturation occurred in multi-pair MIMO relay systems with imperfect CSIT. The use of RSMA in cloud radio access network was considered in [130]. Yu *et al.* proposed an enhanced RSMA technique that outperforms the original RSMA through careful grouping of common signals that are chosen using hierarchical clustering with inter-UEs dissimilarity metric, defined based on channel directions. Additionally, the superiority of RSMA over other MA schemes was investigated for satellite systems in [131], where users achieved max-min fairness for multi-beam satellite

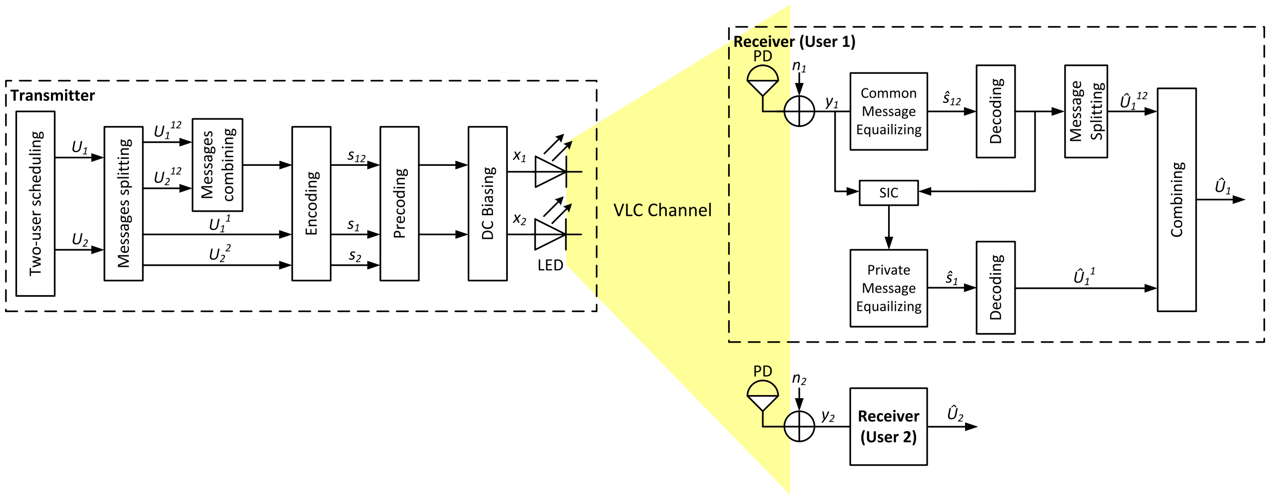


**FIGURE 6.** RSMA-based two-user MISO VLC system.

communications under CSIT uncertainty with minimum inter-beam interference. Finally, RSMA was considered in [132] for cellular-connected drones, where the authors investigated the energy efficiency of RSMA and NOMA schemes in a mmWave downlink transmission scenario.

However, despite the extensive research efforts on RSMA for different systems in the RF domain, its applicability in VLC systems has not yet been explored. Therefore, in this article, we provide preliminary results on the performance of RSMA in VLC systems, and compare its capacity gain with that of existing VLC MA techniques. Furthermore, we give insights into the challenges and future research directions for RSMA-based VLC systems.

### *B. RSMA-BASED VLC*

It is recalled that the concept of RSMA was proposed in the context of a multi-antenna BC channel in [24] to bridge the gap between two extreme MA schemes, namely NOMA and SDMA. Mao *et al.* showed that RSMA works best in the multiple-input case. In the VLC context, this can be realized using several transmitting LEDs to create a BC channel towards several users. Hence, in this survey, we analyze the performance of RSMA in a downlink MU-MISO BC VLC system. To the best of the authors knowledge, such an analysis has not been previously reported in the open technical literature.

#### 1) SYSTEM MODEL

For the sake of simplicity but without loss of generality, we assume two transmitting LEDs that send messages to two single-PD users, as depicted in Fig. 6. It is recalled that RSMA enables the decoding of part of the incurred interference while it treats the remaining part as noise, encompassing in practice SDMA and NOMA schemes as special cases. In order to achieve this, messages $U_1$ and $U_2$ which are intended to users 1 and 2, respectively, are divided into two distinct parts. Specifically, $U_1$ is divided into the private part $U_1^1$ that is decoded only by user 1 and the common part $U_1^{12}$. Similarly, $U_2$ is divided into the private part $U_2^2$ which is decoded only by user 2 and the common part $U_2^{12}$. Then, the two private messages, $U_1^1$ and $U_2^2$, are encoded into distinct private streams $s_1$ and $s_2$, respectively. Then, from a common codebook, $U_1^{12}$ and $U_2^{12}$ are multiplexed and encoded into a common stream $s_{12}$ that will be decoded by both users, which are equipped with SIC for interference mitigation. Without loss of generality, we assume that $s_i$ ($i \in \{1, 2, 12\}$) is randomly selected from a pulse amplitude modulation constellation also with zero mean and normalized range $\{-1, 1\}$. Let $\mathbf{s} = [s_1, s_2, s_{12}]^T$ be the transmitted symbols vector, with $\mathbb{E}(\mathbf{s}\mathbf{s}^T) = \mathbf{I}$. It is further assumed that the non-linear response of the LED is compensated through digital pre-disposition [133]. To reduce MUI, a linear precoding matrix $\mathbf{P} = [\mathbf{p}_1, \mathbf{p}_2, \mathbf{p}_{12}]$ is considered, where $\mathbf{p}_i = [p_{i,1}\ p_{i,2}]^T \in \mathbb{R}_{2\times 1}$ is the precoding vector for the $i^{th}$ stream. A DC bias $\mathbf{d}_{DC} \in \mathbb{R}_{2\times 1}$ is added in order to ensure positive signals, which is required by the LEDs. Hence, the transmitted signal, $\mathbf{x} \in \mathbb{R}^+_{2\times 1}$, can be written as

$$\mathbf{x} = [x_1, x_2]^T = \mathbf{P}\mathbf{s} + \mathbf{d}_{DC} = \sum_{i\in\{1,2,12\}} \mathbf{p}_i s_i + \mathbf{d}_{DC} \quad (10)$$

and the received signal at the $k^{th}$ PD, after optical-to-electrical conversion, is expressed as

$$y_k = \varsigma\zeta \mathbf{h}_k^T \mathbf{x} + n_k, \ \forall k \in \{1, 2\} \quad (11)$$

where $\varsigma$ is the conversion factor of any LED, $\zeta$ is the responsivity of any PD, $\mathbf{h}_k = [h_{k,1}, h_{k,2}]^T$ is the DC channel gain vector between the $k^{th}$ PD and the transmitting LEDs, where each element is expressed as given in (9), and $n_k \sim \mathcal{N}(0, \sigma_k^2)$ is the additive white Gaussian noise, representing the thermal and shot noises, with zero-mean and variance $\sigma_k^2$. Due to the low mobility of indoor users, we assume that the channel gains are constant during the transmission, and that perfect CSI is available at the transmitter. In order to accurately design the precoding matrix $\mathbf{P}$, the following constraints need to be satisfied to ensure that the LEDs work in their dynamic range

$$L_1(\boldsymbol{p}_l) = \sum_{i\in 1,2,12} |p_{l,i}| \\ = \min\left(d_{DC}, P_{max} - d_{DC}\right), \ \forall l \in \{1,2\} \tag{12}$$

where $\boldsymbol{p}_l$ is the $l^{th}$ row of the precoding matrix $\mathbf{P}$.

The MMSE equalizer for the common stream is utilized at the $k^{th}$ user for signal detection [96], followed by SIC as follows: First, user $k$ decodes the common signal $s_{12}$ while treating the other signals as noise. Hence, the received SINR at the $k^{th}$ user, for the common signal, is expressed as

$$\gamma_k^{12} = \frac{\left(\mathbf{h}_k^T \mathbf{p}_{12}\right)^2}{\left(\mathbf{h}_k^T \mathbf{p}_1\right)^2 + \left(\mathbf{h}_k^T \mathbf{p}_2\right)^2 + \hat{\sigma}_k^2}, \ \forall k \in \{1,2\} \tag{13}$$

where $\hat{\sigma}_k^2 = \sigma_k^2/(\varsigma\zeta)^2$ is the normalized received noise power. For the sake of simplicity, we assume that $\varsigma\zeta = 1$, and thus $\hat{\sigma}_k^2 = \sigma_k^2$. Then, the effect of the common signal is removed using SIC. This allows for the detection of the private signal by first employing the MMSE equalizer, and then user $k$ attempts to decode its private message $s_k$, while treating the private signals of other users as noise. Consequently, the received SINR at user $k$, for its private signal, can be written as

$$\gamma_k^k = \frac{\left(\mathbf{h}_k^T \mathbf{p}_k\right)^2}{\left(\mathbf{h}_k^T \mathbf{p}_{\bar{k}}\right)^2 + \sigma_k^2}, \ \forall (k,\bar{k}) \in \{(1,2),(2,1)\} \tag{14}$$

and the achieved data rate at user $k$ is expressed by [24]

$$R_k^{12} = \log_2(1 + \gamma_k^{12}), \tag{15}$$

and

$$R_k^k = \log_2(1 + \gamma_k^k), \ \forall k \in \{1,2\} \tag{16}$$

where $R_k^{12}$ and $R_k^k$ are the data rates for the common and private signals, respectively. In order to ensure successful decoding of the common stream $s_{12}$ at both users, the common rate shall not exceed $R_{12} = \min(R_1^{12}, R_2^{12})$. It is also noted that the targeted common rate for each user can be achieved if $R_{12}$ is adequately shared between the two users, i.e., $R_{12} = \sum_{k=1}^{2} R_{k,com}$, where $R_{k,com}$ is the $k^{th}$ user portion of the common rate. Consequently, the total achievable data rate of user $k$, denoted $R_{k,ov}$, can be expressed by [24]

$$R_{k,ov} = R_{k,com} + R_k^k, \ \forall k \in \{1,2\}. \tag{17}$$

#### 2) PROBLEM FORMULATION

Although conventional precoders, such as ZF and ZF-DPC, are simple and can efficiently remove MUI, they suffer from performance degradation at low SNR values. Consequently, there is a need for an optimal precoding in order to maximize an objective function, e.g., sum rate, weighted sum rate (WSR), proportional fairness, or max-min fairness [98], under QoS requirements and per-LED transmit power constraints to take into account the nature of the optical signals, which are real and positive valued. Inspired by the MMSE precoding method presented in [134], we maximize the WSR of the investigated MU-MISO VLC system. To this end, for a given weights vector $\mathbf{w} = [w_1, w_2]$, the WSR maximization problem (P1) can be expressed as follows:

**Algorithm 1:** Alternating Optimization Algorithm.

1: Initialize $k \leftarrow 0$, $\mathbf{P}[k]$, $R[k]$
2: **repeat**
3: $k \leftarrow k+1$; $\mathbf{P}[k-1] \leftarrow \mathbf{P}$
4: Update the WMMSE weights $\mathbf{w} \leftarrow \mathbf{w}(\mathbf{P}[k-1])$
5: Update the receive filter gains $\boldsymbol{\alpha} \leftarrow \boldsymbol{\alpha}(\mathbf{P}[k-1])$
6: Solve (P1) using WMMSE transformation for updated $(\mathbf{w}, \boldsymbol{\alpha})$, then update $(\mathbf{P}, \mathbf{v})$
7: **until** $|R[k] - R[k-1]| \leq \delta$.

$$\max_{\mathbf{P},\mathbf{R}_{com}} \quad R(\mathbf{w}) = \sum_{k=1}^{2} w_k\, R_{k,ov} \tag{P1}$$

$$\text{s.t.} \quad L_1(\boldsymbol{p}_l) \leq \varepsilon, \ \forall l \in \{1,2\} \tag{P1.a}$$

$$\sum_{k=1}^{2} R_{k,com} \leq R_{12} \tag{P1.b}$$

$$\mathbf{R}_{com} \geq \mathbf{0} \tag{P1.c}$$

where $\mathbf{R}_{com} = [R_{1,com}, R_{2,com}]$ is the common rate vector. Furthermore, P1.a accounts for the optical power constraints associated with the transmitting LEDs, whereas P1.b and P1.c denote the constraints associated with common message rate. It is noted that these constraints are required in order to ensure that the common message is successfully decoded by both users. To this effect, it can be noticed that (P1) is non-convex due to the presence of variables $\mathbf{p}_k$ ($k \in \{1,2\}$) in the denominator of the SINR expressions (13)-(14). Thus, its solution is not straightforward. Similar to [135], we opt for problem reformulation, where the objective function becomes the minimization of the weighted MMSE, and is achieved by jointly optimizing the WMMSE precoding vectors and MSE equalizer weights. To obtain a local optimum, we utilize alternating optimization (AO) detailed in Algorithm 1 [135], where $k$ is the iteration index, $\mathbf{w}$ is the MMSE weights vector, $\boldsymbol{\alpha}$ is the MSE receiver weights vector, $\mathbf{v}$ is the transformation of $\mathbf{R}_{com}$, and $\delta$ is the tolerance threshold. In order to converge to a maximum WSR, the algorithm alternates between WMMSE precoding design and MSE equalizer weights design.[4] Finally, the reformulated problem can be solved using optimization tools such as CVX in MATLAB [136]. It is noted that the AO algorithm converges faster and achieves better performance

[4]For further details on the AO procedure, we refer the reader to Sections IV and V in [135].

than other types of precoding optimization algorithms. However, its complexity increases with the number of users.

### 3) NOMA AND SDMA AS SPECIAL CASES OF RSMA

As already mentioned, RSMA is a generalized MA scheme that includes NOMA and SDMA as special cases. To implement SDMA from RSMA, the common stream is allocated null power, and each user's message is encoded only as a private stream. Hence, the transmitted signal in this case is

$$\mathbf{x} = \mathbf{Ps} + \mathbf{d}_{DC} = \sum_{i\in\{1,2\}} \mathbf{p}_i s_i + \mathbf{d}_{DC} \tag{19}$$

and the received SINR at each user simplifies into (14). Similarly, NOMA can be obtained from RSMA by encoding one of the users' messages as a private stream, i.e., the user with the strongest channel, and the signal of the second user is encoded as a common stream. Assuming that user 1 has the strongest channel gain, then the transmitted signal in this case can be written as

$$\mathbf{x} = \mathbf{Ps} + \mathbf{d}_{DC} = \sum_{i\in\{1,12\}} \mathbf{p_i} s_i + \mathbf{d}_{DC} \tag{20}$$

and the associated SINRs of the first and second users are given by

$$\gamma_1^1 = \frac{(\mathbf{h}_1^T\mathbf{p}_1)^2}{\sigma_1^2} \tag{21}$$

and

$$\gamma_2^{12} = \min\left(\frac{(\mathbf{h}_1^T\mathbf{p}_{12})^2}{(\mathbf{h}_1^T\mathbf{p}_1)^2+\sigma_1^2}, \frac{(\mathbf{h}_2^T\mathbf{p}_{12})^2}{(\mathbf{h}_2^T\mathbf{p}_1)^2+\sigma_2^2}\right) \tag{22}$$

respectively. It is worth mentioning that the flexibility of RSMA comes at the expense of a slightly higher encoding complexity at the transmitter.

## VI. PERFORMANCE EVALUATION

This section presents different scenarios for the application of RSMA in VLC systems, where we investigate their performance in terms of WSR, and then compare them with SDMA and NOMA schemes. Moreover, we study the impact of different users' locations within an indoor space.

We consider an RSMA-based MU-MISO VLC system, where two single-PD users are served by two or four LED fixtures in a room of size $5 \times 5 \times 4\ m^3$. The room configurations with the users' scenarios are detailed in Figs. 7–8, as follows: In both figures, the main two users' location scenarios are considered. In the first (blue circles), users are located in the middle space of the room with a separation of 3 m, whereas in the second (green circles), users are located in the top of the room, with a smaller separation of 0.4 m. Between the two figures, the number and locations of LEDs is varied from 4 to 2. In addition, a third scenario is considered for the 4 LEDs case, where the separation between users is 0.94 m (yellow circle for user 1 and green circle of user 2). All coordinates are expressed in the 3D-space system. Furthermore, we assume the same optical devices characteristics as in [96], while the

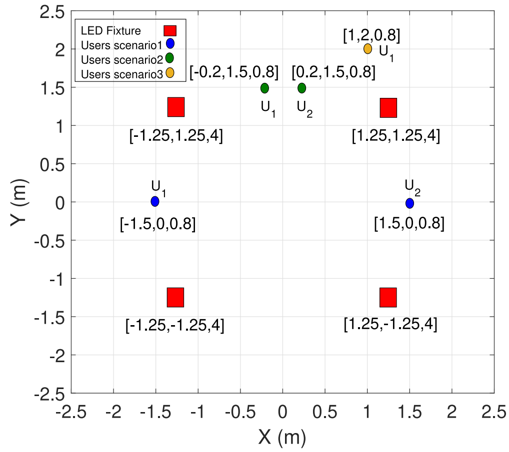


**FIGURE 7.** Room configuration and users' scenarios (4 LEDs).

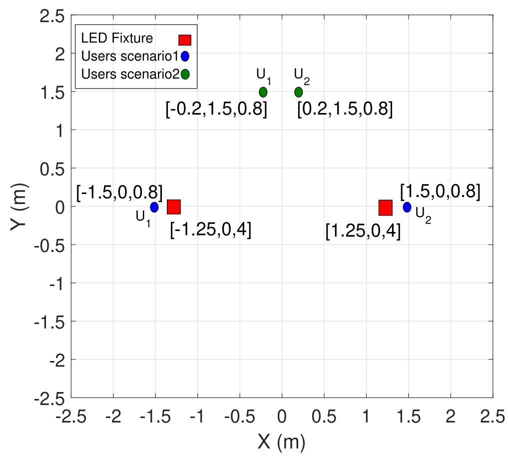


**FIGURE 8.** Room configuration and users' scenarios (2 LEDs).

**TABLE 4.** Simulation Parameters

| Parameter | Symbol | Value |
|---|---|---|
| Number of LEDs per fixture | $Q$ | $3600\ (60\times 60)$ |
| LED beam angle | $\varphi_{1/2}$ | $60^o$ |
| PD area | $A_k\ (k=1,2)$ | $1\ cm^2$ |
| Refractive index of PD | $n$ | 1.5 |
| Gain of optical filter | $T_s(\phi_{k,i})\ (k=1,2)$ | 1 |
| FoV of PD | $\phi_c$ | $60^o$ |

two users are allocated equal priority, i.e., $w_1 = w_2 = \frac{1}{2}$ in the objective function of (P1). Also, since the noise power is assumed to be unity, then the SNR designates the transmit power per-LED. The remaining parameters are detailed in Table 4.

Fig. 9 shows the WSR performance for RSMA, NOMA and SDMA, in "Scenario 1, 4 LEDs". It can be seen that RSMA outperforms both NOMA and SDMA, particularly at high SNR. In addition, SDMA performs better than NOMA, since the number of transmitter LEDs is larger than the number of users, allowing efficient management of MUI. However, SDMA performs worse than RSMA due to the difficult

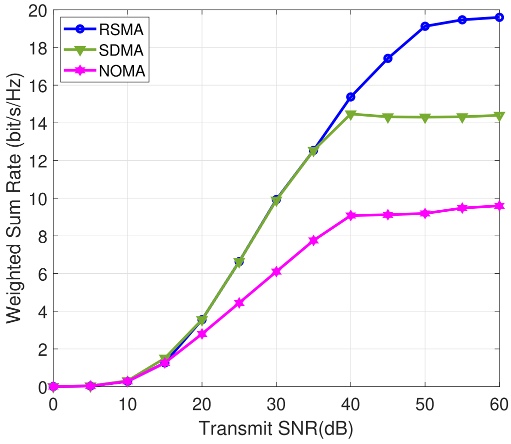


**FIGURE 9.** WSR vs. SNR per LED array (Scenario 1, 4 LEDs).

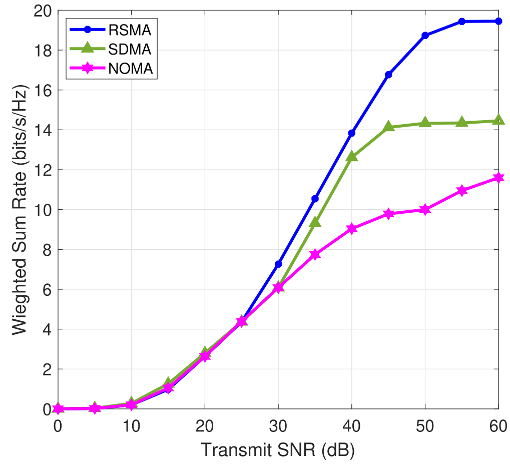


**FIGURE 11.** WSR vs. SNR per LED array (Scenario 3, 4 LEDs).

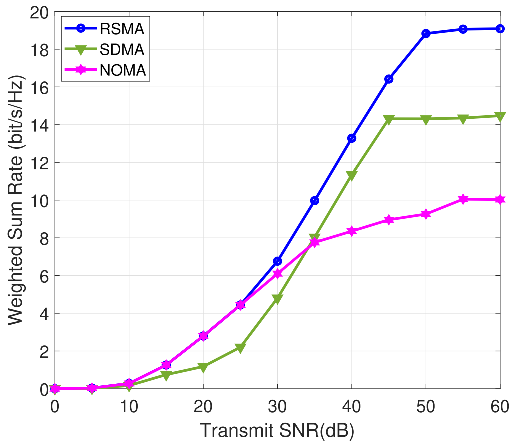


**FIGURE 10.** WSR vs. SNR per LED array (Scenario 2, 4 LEDs).

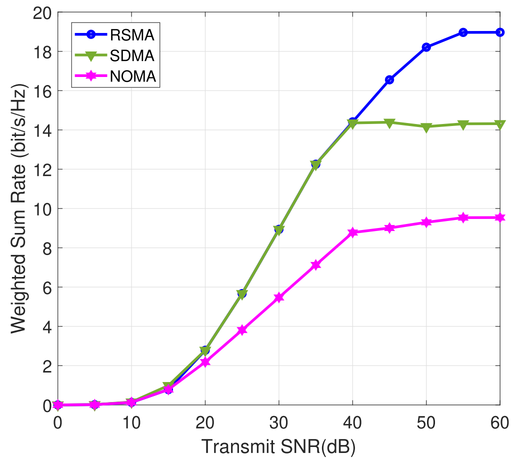


**FIGURE 12.** WSR vs. SNR per LED array (Scenario 1, 2 LEDs).

channels alignment between users, caused by the nature of the VLC channel. In Fig. 10, the same comparison is made for "Scenario 2, 4 LEDs". With a smaller separation between users, channels are more correlated, which is reflected by the corresponding achievable performance. For instance, using RSMA, WSR=13 bits/s/Hz (RSMA) is achieved at SNR=40 dB, compared to WSR=15.5 bits/s/Hz in Fig. 9. Nevertheless, the performance of RSMA still exceeds that of both NOMA and SDMA. It is also observed that for SNRs below 35 dB, NOMA outperforms SDMA, which shows that NOMA is able to distinguish different users using precoding and SIC receivers. However, for SNRs above 35 dB, this procedure is less effective, and direct beamforming using SDMA becomes privileged. Consequently, NOMA is favored at lower SNRs for low separation between users, whilst SDMA is more performant for high SNRs. Next we examine the impact of the users separation, i.e., channels correlation of different users. To this end, Fig. 11 illustrates the WSR performance for "Scenario 3" ($U_1$ yellow + $U_2$ green in Fig. 7), where the users separation is 0.94 m. It can be seen that the WSR performance of NOMA is improved compared to "Scenario 2." This is due to the reduced channel correlation between the two users, since the separating distance between users increased from 0.4 m to 0.94 m. Furthermore, SDMA and RSMA demonstrate improved performances, compared to "Scenario 2," due to the lower interference between users.

In Figs. 12–13, we consider the same scenarios, but with 2 LEDs. Similar to the previous results, the superiority of RSMA in terms of WSR over the other techniques is clearly illustrated, whilst the performance of SDMA is slightly degraded due to the smaller number of LEDs. Similar to Fig. 10, in Fig. 13 the SDMA performance is degraded at SNRs below 36 dB compared to NOMA, but outperforms the latter as the SNR increases. Finally, Fig. 14 illustrates the users' locations impact on the WSR performance of the RSMA scheme. There, we consider the room setup of 2 LEDs, and two users initially located in the middle of the room. Based on this, the first and second users move to the east and west walls at the same constant speed, respectively. Thus, their physical separation increases until reaching its maximum 5 m (i.e., users have reached the opposite walls). To this effect, it can be seen that

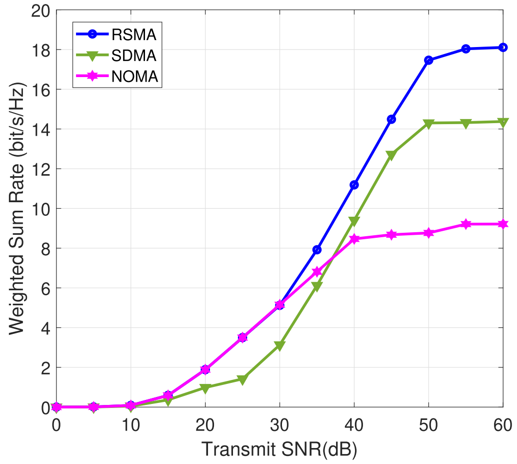


**FIGURE 13.** WSR vs. SNR per LED array (Scenario 2, 2 LEDs).

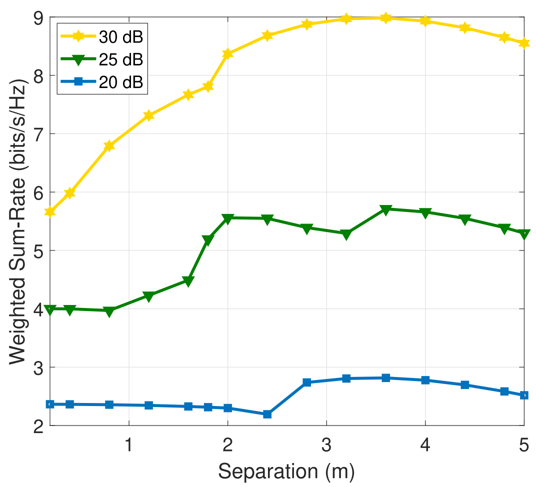


**FIGURE 14.** Performance of RSMA for different users locations/separations and SNRs.

WSR varies with the separation, until a maximum value is achieved for a separation equal to 3.6 m. This corresponds to users' locations [-1.8, 0, 0.8] and [1.8, 0, 0.8], where the correlation between channels is low, but users are very close to one of the serving LEDs to capture maximal power. However, as this separation increases above 3.6 m, the WSR degrades due to longer distances between the users and LEDs. It can be seen that these optimal users' locations are the same for different SNRs. Consequently, designing indoor spaces using RSMA-VLC requires a thorough consideration of the LEDs' and users' locations.

## VII. OPEN ISSUES AND RESEARCH DIRECTIONS

In this paper, we reviewed different MA techniques that have been proposed for improving the spectral efficiency of VLC systems and minimize the encountered VLC-specific interference issues. Then, we addressed a preliminary work on the utilization of RSMA in VLC systems. It has been shown that RSMA is a powerful MA scheme that can provide high data rates and reliable VLC communications. However, several associated issues need to be addressed and analyzed for the practical realization of RSMA-VLC. For instance, the impact of the non-linear distortion caused by the different circuits components, such as LEDs, PDs, and analog/digital and digital/analog converters has to be thoroughly quantified. Moreover, as a novel MA technique, more efforts are required to study the design of the physical and MAC layers. Hence, different performance metrics, modulation and coding schemes, and security issues, are open research problems in RSMA-based VLC systems. Additionally, optimal precoding and power allocation for RSMA-VLC are still open for investigation, where new linear and non-linear techniques can be proposed and optimized. Moreover, the current literature has mainly focused on the Gaussian noise assumption, but neglected the effect of ambient light, which can cause a degradation in the overall system performance.

Other current assumptions include: the receiver is always pointing upward, a LoS is always available and CSI is perfectly known. However, this may not be the case in practical communication scenarios, where the receiver can be differently oriented, the VLC link may experience shadowing and/or blockage, and CSI knowledge can realistically be imperfect and/or outdated. Consequently, the design and performance evaluation of RSMA-VLC systems that take into account these practical constraints is to be studied. In this context, innovative solutions to circumvent the absence of a LoS may include enabling optical cooperative communications and device-to-device (D2D) communications. Indeed, optical cooperation among VLC transmitters guarantees reliable transmissions to users in a specific area [20], whereas in D2D communications, users with strong VLC links may assist forwarding data to users with blocked VLC channels [137]. Also, taking into consideration the QoS requirements of different users during the design of such systems is likely to lead to overall improved achievable performance levels. Finally, the analysis of massive MIMO RSMA-VLC systems is another interesting open research problem.

## VIII. CONCLUSION

In this paper, we provided an extensive review on several MA schemes for MIMO-VLC systems, which includes a detailed coverage of the their advantages and limitations. The review covered the NOMA and SDMA integration into VLC systems, and showed how they minimize VLC interference and improve the overall communication performance. In addition, we reviewed RSMA for RF systems, and demonstrated it as a generalizing multiple access of NOMA and SDMA. Subsequently, we presented a preliminary study for the integration of RSMA into VLC systems, taking into consideration the per-LED power constraints. The SINR and WSR expressions are obtained for a two-user MISO VLC system, and results showed the flexibility of RSMA in generalizing NOMA and

SDMA, at slightly increased design complexity. Through extensive computer simulations, we showed that RSMA-VLC outperforms both NOMA and SDMA in terms of achievable WSR. Also, it was shown that RSMA is robust against channel correlation, and hence, it is considered as a particularly suitable MA candidate for VLC in beyond 5 G networks. Finally, a number of related open issues and thoroughly research directions linked to MIMO RSMA-VLC, have been presented and discussed.

## REFERENCES

[1] T. Komine and M. Nakagawa, "Fundamental analysis for visible-light communication system using LED lights," *IEEE Trans. Consum. Electron.*, vol. 50, no. 1, pp. 100–107, Feb. 2004.
[2] H. Elgala, R. Mesleh, and H. Haas, "Indoor optical wireless communication: Potential and state-of-the-art," *IEEE Commun. Mag.*, vol. 49, no. 9, pp. 56–62, Sep. 2011.
[3] Z. Ghassemlooy, W. Popoola, and S. Rajbhandari, *Optical Wireless Communication: System Channel Modelling MATLAB*, 2nd ed., Boca Raton, FL, USA: CRC Press, May 2019.
[4] A. R. Ndjiongue, T. M. N. Ngatched, O. A. Dobre, and A. G. Armada, "VLC-based networking: Feasibility and challenges," *IEEE Netw.*, vol. 34, no. 4, pp. 158–165, Jul./Aug. 2020.
[5] L. Grobe *et al.*, "High-speed visible light communication systems," *IEEE Commun. Mag.*, vol. 51, no. 12, pp. 60–66, Dec. 2013.
[6] D. Karunatilaka, F. Zafar, V. Kalavally, and R. Parthiban, "LED based indoor visible light communications: State of the art," *IEEE Commun. Surv. Tuts.*, vol. 17, no. 3, pp. 1649–1678, Jul.-Sep. 2015.
[7] F. Miramirkhani and M. Uysal, "Channel modeling and characterization for visible light communications," *IEEE Photon. J.*, vol. 7, no. 6, pp. 1–16, Dec. 2015.
[8] IEEE, "IEEE draft standard for local and metropolitan area networks - Part 15.7: Short-range optical wireless communications," *IEEE P802.15.7/D3, Aug. 2018*, pp. 1–412, Sep. 2018.
[9] V. K. Papanikolaou, P. D. Diamantoulakis, P. C. Sofotasios, S. Muhaidat, and G. K. Karagiannidis, "On optimal resource allocation for hybrid VLC/RF networks with common backhaul," *IEEE Trans. Cogn. Commun. Netw.*, vol. 6, no. 1, pp. 352–365, Mar. 2020.
[10] A. Jovicic, J. Li, and T. Richardson, "Visible light communication: Opportunities, challenges and the path to market," *IEEE Commun. Mag.*, vol. 51, no. 12, pp. 26–32, Dec. 2013.
[11] P. H. Pathak, X. Feng, P. Hu, and P. Mohapatra, "Visible light communication, networking, and sensing: A survey, potential and challenges," *IEEE Commun. Surv. Tuts.*, vol. 17, no. 4, pp. 2047–2077, Oct.-Dec. 2015.
[12] H. Yang, C. Chen, W. Zhong, and A. Alphones, "Joint precoder and equalizer design for multi-user multi-cell MIMO VLC systems," *IEEE Trans. Veh. Technol.*, vol. 67, no. 12, pp. 11 354–11 364, Dec. 2018.
[13] F. Ahmed, A. A. Dowhuszko, and O. Tirkkonen, "Self-organizing algorithms for interference coordination in small cell networks," *IEEE Trans. Veh. Technol.*, vol. 66, no. 9, pp. 8333–8346, Sep. 2017.
[14] M. Kashef, M. Abdallah, K. Qaraqe, H. Haas, and M. Uysal, "Coordinated interference management for visible light communication systems," *IEEE/OSA J. Opt. Commun. Netw.*, vol. 7, no. 11, pp. 1098–1108, Nov. 2015.
[15] R. Bai, H. Tian, B. Fan, and S. Liang, "Coordinated transmission based interference mitigation in vlc network," in *Proc. IEEE 82nd Veh. Technol. Conf.*, 2015, pp. 1–5.
[16] K. Zhou, C. Gong, and Z. Xu, "Color planning and intercell interference coordination for multicolor visible light communication networks," *J. Lightw. Technol.*, vol. 35, no. 22, pp. 4980–4993, Nov. 2017.
[17] S. Jung, D. Kwon, S. Yang, and S. Han, "Reduction of inter-cell interference in asynchronous multi-cellular VLC by using OFDMA-based cell partitioning," in *Proc. 18th Int. Conf. Transp. Opt. Netw.*, 2016, pp. 1–4.
[18] C. Chen, W. Zhong, H. Yang, S. Zhang, and P. Du, "Reduction of sinr fluctuation in indoor multi-cell VLC systems using optimized angle diversity receiver," *J. Lightw. Technol.*, vol. 36, no. 17, pp. 3603–3610, 2018.
[19] H. Ryoo, D. Kwon, S. Yang, and S. Han, "Differential optical detection in vlc for inter-cell interference reduced flexible cell planning," *IEEE Photon. Technol. Lett.*, vol. 28, no. 23, pp. 2728–2731, Dec. 2016.
[20] T. V. Pham and A. T. Pham, "Coordination/cooperation strategies and optimal zero-forcing precoding design for multi-user multi-cell VLC networks," *IEEE Trans. Commun.*, vol. 67, no. 6, pp. 4240–4251, Jun. 2019.
[21] J. Armstrong, "OFDM for optical communications," *J. Lightw Technol.*, vol. 27, no. 3, pp. 189–204, Feb. 2009.
[22] J. A. Salehi, "Code division multiple-access techniques in optical fiber networks. Part I. Fundamental principles," *IEEE Trans. Commun.*, vol. 37, no. 8, pp. 824–833, Aug. 1989.
[23] Z. Ding, Z. Yang, P. Fan, and H. V. Poor, "On the performance of non-orthogonal multiple access in 5G systems with randomly deployed users," *IEEE Signal Process. Lett.*, vol. 21, no. 12, pp. 1501–1505, Dec. 2014.
[24] Y. Mao, B. Clerckx, and V. Li, "Rate-splitting multiple access for downlink communication systems: Bridging, generalizing, and outperforming SDMA and NOMA," *EURASIP J. Wireless Commun. Netw.*, no. 133, pp. 1–54, May 2018.
[25] S. S. Bawazir, P. C. Sofotasios, S. Muhaidat, Y. Al Hammadi, and G. K. Karagiannidis, "Multiple access for visible light communications: Research challenges and future trends," *IEEE Access*, vol. 6, pp. 26 167–26 174, May 2018.
[26] M. Vaezi, G. A. Aruma Baduge, Y. Liu, A. Arafa, F. Fang, and Z. Ding, "Interplay between NOMA and other emerging technologies: A survey," *IEEE Trans. Cogn. Commun. Netw..*, vol. 5, no. 4, pp. 900–919, Dec. 2019.
[27] M. Obeed, A. M. Salhab, M. Alouini, and S. A. Zummo, "On optimizing VLC networks for downlink multi-user transmission: A survey," *IEEE Commun. Surv. Tuts.*, vol. 21, no. 3, pp. 2947–2976, Jul.-Sep. 2019.
[28] M. Sze and K. Ng, *Phys. Semicond. Devices*, Hoboken, NJ, USA: John Wiley and Sons Inc., 2007.
[29] E. Monteiro and S. Hranilovic, "Design and implementation of color-shift keying for visible light communications," *J. Lightw. Technol.*, vol. 32, no. 10, pp. 2053–2060, May 2014.
[30] L. Dai, B. Wang, Y. Yuan, S. Han, C. I, and Z. Wang, "Non-orthogonal multiple access for 5G: Solutions, challenges, opportunities, and future research trends," *IEEE Commun. Mag.*, vol. 53, no. 9, pp. 74–81, Sep. 2015.
[31] H. Marshoud, V. M. Kapinas, G. K. Karagiannidis, and S. Muhaidat, "Non-orthogonal multiple access for visible light communications," *IEEE Photon. Technol. Lett.*, vol. 28, no. 1, pp. 51–54, Jan. 2016.
[32] R. Mesleh, H. Elgala, and H. Haas, "On the performance of different OFDM based optical wireless communication systems," *IEEE/OSA J. Opt. Commun. and Netw..*, vol. 3, no. 8, pp. 620–628, Aug. 2011.
[33] E. Giacoumidis *et al.*, "Extensive comparisons of optical fast-OFDM and conventional optical OFDM for local and access networks," *IEEE/OSA J. Opt. Commun. Netw.*, vol. 4, no. 10, pp. 724–733, Oct. 2012.
[34] S. D. Dissanayake and J. Armstrong, "Comparison of ACO-OFDM, DCO-OFDM and ADO-OFDM in IM/DD systems," *J. Lightw. Technol.*, vol. 31, no. 7, pp. 1063–1072, Apr. 2013.
[35] H. Elgala and T. D. C. Little, "Polar-based OFDM and SC-FDE links toward energy-efficient Gbps transmission under IM-DD optical system constraints [Invited]," *IEEE/OSA J. Opt. Commun. Netw..*, vol. 7, no. 2, pp. A277–A284, Feb. 2015.
[36] S. Ali, E. Hossain, and D. I. Kim, "Non-orthogonal multiple access (NOMA) for downlink multiuser MIMO systems: User clustering, beamforming, and power allocation," *IEEE Access*, vol. 5, pp. 565–577, Jan. 2017.
[37] F. Wei, W. Chen, Y. Wu, J. Li, and Y. Luo, "Toward 5G wireless interface technology: Enabling nonorthogonal multiple access in the sparse code domain," *IEEE Veh. Technol. Mag.*, vol. 13, no. 4, pp. 18–27, Dec. 2018.
[38] S. M. R. Islam, N. Avazov, O. A. Dobre, and K. Kwak, "Power-domain non-orthogonal multiple access (NOMA) in 5G systems: Potentials and challenges," *IEEE Commun. Surv. Tuts.*, vol. 19, no. 2, pp. 721–742, Apr.-Jun. 2017.
[39] M. H. Shoreh, A. Fallahpour, and J. A. Salehi, "Design concepts and performance analysis of multicarrier CDMA for indoor visible light communications," *IEEE/OSA J. Opt. Commun. Netw..*, vol. 7, no. 6, pp. 554–562, Jun. 2015.

[40] Y. Chen, Y. Chang, Y. Tseng, and W. Chen, “A framework for simultaneous message broadcasting using CDMA-based visible light communications,” *IEEE Sensors J.*, vol. 15, no. 12, pp. 6819–6827, Dec. 2015.

[41] J. Dai, K. Niu, and J. Lin, “Code-domain non-orthogonal multiple access for visible light communications,” in *Proc. IEEE Globecom. Workshops.*, Dec. 2018, pp. 1–6.

[42] S. Lou, C. Gong, Q. Gao, and Z. Xu, “SCMA with low complexity symmetric codebook design for visible light communication,” in *Proc. IEEE Int. Conf. Commun.*, May 2018, pp. 1–6.

[43] C. Rashidi, S. Aljunid, F. Ghani, H. A. Fadhil, and M. Anuar, “New design of flexible cross correlation (FCC) code for SAC-OCDMA system,” *Procedia Eng.*, vol. 53, pp. 420–427, Mar. 2013.

[44] R. Razavi, R. Hoshyar, M. A. Imran, and Y. Wang, “Information theoretic analysis of LDS scheme,” *IEEE Commun. Lett.*, vol. 15, no. 8, pp. 798–800, Aug. 2011.

[45] M. Al-Imari, M. A. Imran, R. Tafazolli, and D. Chen, “Subcarrier and power allocation for LDS-OFDM system,” in *Proc. IEEE 73rd Veh. Technol. Conf.*, 2011, pp. 1–5.

[46] Y. Cai, Z. Qin, F. Cui, G. Y. Li, and J. A. McCann, “Modulation and multiple access for 5G networks,” *IEEE Commun. Surv. Tuts.*, vol. 20, no. 1, pp. 629–646, Jan.-Mar. 2018.

[47] S. Tao, Y. Zuo, H. Yu, Q. Li, and Y. Tang, “Power allocation of non-orthogonal multiple access with variable on-off keying dimming control in visible light communication networks,” in *Proc. IEEE Int. Conf. Commun. Tech.*, Nov. 2018, pp. 321–325.

[48] Y. Cai, Z. Qin, F. Cui, G. Y. Li, and J. A. McCann, “Modulation and multiple access for 5G networks,” *IEEE Commun. Surv. Tut.*, vol. 20, no. 1, pp. 629–646, Jan.–Mar. 2018.

[49] S. Al Ahmadi, O. Maraqa, M. Uysal, and S. M. Sait, “Multi-user visible light communications: State-of-the-Art and future directions,” *IEEE Access*, vol. 6, pp. 70 555–70 571, Nov. 2018.

[50] G. Pan, H. Lei, Z. Ding, and Q. Ni, “3-d hybrid VLC-RF indoor iot systems with light energy harvesting,” *IEEE Trans. Green Commun. and Netw.*, vol. 3, no. 3, pp. 853–865, Sep. 2019.

[51] M. T. Alresheedi, A. T. Hussein, and J. M. H. Elmirghani, “Uplink design in VLC systems with ir sources and beam steering,” *IET Commun.*, vol. 11, no. 3, pp. 311–317, 2017.

[52] H. Marshoud, S. Muhaidat, P. C. Sofotasios, S. Hussain, M. A. Imran, and B. S. Sharif, “Optical non-orthogonal multiple access for visible light communication,” *IEEE Wireless Commun.*, vol. 25, no. 2, pp. 82–88, Apr. 2018.

[53] H. Marshoud, P. C. Sofotasios, S. Muhaidat, G. K. Karagiannidis, and B. S. Sharif, “On the performance of visible light communication systems with non-orthogonal multiple access,” *IEEE Trans. Wireless Commun.*, vol. 16, no. 10, pp. 6350–6364, Oct. 2017.

[54] C. Wang, Y. He, F. R. Yu, Q. Chen, and L. Tang, “Integration of networking, caching, and computing in wireless systems: A survey, some research issues, and challenges,” *IEEE Commun. Surv. Tuts.*, vol. 20, no. 1, pp. 7–38, Jan.-Mar. 2018.

[55] T. Cover, “Broadcast channels,” *IEEE Trans. Inf. Theory*, vol. 18, no. 1, pp. 2–14, Jan. 1972.

[56] B. Lin, X. Tang, and Z. Ghassemlooy, “Optical power domain NOMA for visible light communications,” *IEEE Wireless Commun. Lett.*, vol. 8, no. 4, pp. 1260–1263, Aug. 2019.

[57] X. Liu, Z. Chen, Y. Wang, F. Zhou, Y. Luo, and R. Q. Hu, “BER analysis of NOMA-enabled visible light communication systems with different modulations,” *IEEE Trans. Veh. Technol.*, vol. 68, no. 11, pp. 10 807–10 821, Nov. 2019.

[58] R. C. Kizilirmak, C. R. Rowell, and M. Uysal, “Non-orthogonal multiple access (NOMA) for indoor visible light communications,” in *Proc. 4th Int. Wrkshp. Opt. Wireless Commun.*, Sep. 2015, pp. 98–101.

[59] L. Yin, W. O. Popoola, X. Wu, and H. Haas, “Performance evaluation of non-orthogonal multiple access in visible light communication,” *IEEE Trans. Commun.*, vol. 64, no. 12, pp. 5162–5175, Dec. 2016.

[60] Z. Yang, W. Xu, and Y. Li, “Fair non-orthogonal multiple access for visible light communication downlinks,” *IEEE Wireless Commun. Lett.*, vol. 6, no. 1, pp. 66–69, Feb. 2017.

[61] H. Shen, Y. Wu, W. Xu, and C. Zhao, “Optimal power allocation for downlink two-user non-orthogonal multiple access in visible light communication,” *J. Commun. Inf. Net.*, vol. 2, no. 4, pp. 57–64, Dec. 2017.

[62] Y. Yapici and I. Guvenc, “NOMA for VLC downlink transmission with random receiver orientation,” *IEEE Trans. Commun.*, vol. 67, no. 8, pp. 5558–5573, Aug. 2019.

[63] W. Chu, J. Dang, Z. Zhang, and L. Wu, “Effect of clipping on the achievable rate of non-orthogonal multiple access with DCO-OFDM,” in *Proc. 9th Int. Conf. Wireless Commun. Signal Process.*, Oct. 2017, pp. 1–6.

[64] Y. Fu, Y. Hong, L. Chen, and C. W. Sung, “Enhanced power allocation for sum rate maximization in OFDM-NOMA VLC systems,” *IEEE Photon. Technol. Lett.*, vol. 30, no. 13, pp. 1218–1221, Jul. 2018.

[65] X. Guan, Q. Yang, and C. Chan, “Joint detection of visible light communication signals under non-orthogonal multiple access,” *IEEE Photon. Technol. Lett.*, vol. 29, no. 4, pp. 377–380, Feb. 2017.

[66] A. Wyner, “Recent results in the Shannon theory,” *IEEE Trans. Inf. Theory*, vol. 20, no. 1, pp. 2–10, Jan. 1974.

[67] V. Nguyen, H. D. Tuan, T. Q. Duong, H. V. Poor, and O. Shin, “Precoder design for signal superposition in MIMO-NOMA multicell networks,” *IEEE J. Sel. Areas Commun.*, vol. 35, no. 12, pp. 2681–2695, Dec. 2017.

[68] S. M. R. Islam, M. Zeng, O. A. Dobre, and K. Kwak, “Resource allocation for downlink NOMA systems: Key techniques and open issues,” *IEEE Wireless Commun.*, vol. 25, no. 2, pp. 40–47, Apr. 2018.

[69] M. Zeng, A. Yadav, O. A. Dobre, G. I. Tsiropoulos, and H. V. Poor, “Capacity comparison between MIMO-NOMA and MIMO-OMA with multiple users in a cluster,” *IEEE J. Sel. Areas Commun.*, vol. 35, no. 10, pp. 2413–2424, Oct. 2017.

[70] M. Zeng, A. Yadav, O. A. Dobre, G. I. Tsiropoulos, and H. V. Poor, “On the sum rate of MIMO-NOMA and MIMO-OMA systems,” *IEEE Wireless Commun. Lett.*, vol. 6, no. 4, pp. 534–537, Aug. 2017.

[71] Z. Ding, F. Adachi, and H. V. Poor, “The application of MIMO to non-orthogonal multiple access,” *IEEE Trans. Wireless Commun.*, vol. 15, no. 1, pp. 537–552, Jan. 2016.

[72] Z. Ding, R. Schober, and H. V. Poor, “A general MIMO framework for NOMA downlink and uplink transmission based on signal alignment,” *IEEE Trans. Wireless Commun.*, vol. 15, no. 6, pp. 4438–4454, Jun. 2016.

[73] M. Morales-Céspedes, O. A. Dobre, and A. García-Armada, “Semi-blind interference aligned NOMA for downlink MU-MISO systems,” *IEEE Trans. Commun.*, vol. 68, no. 3, pp. 1852–1865, Mar. 2020.

[74] C. Chen, W. Zhong, H. Yang, and P. Du, “On the performance of MIMO-NOMA-based visible light communication systems,” *IEEE Photon. Technol. Lett.*, vol. 30, no. 4, pp. 307–310, Feb. 2018.

[75] X. Zhang, Q. Gao, C. Gong, and Z. Xu, “User grouping and power allocation for NOMA visible light communication multi-cell networks,” *IEEE Commun. Lett.*, vol. 21, no. 4, pp. 777–780, Apr. 2017.

[76] V. S. Rajput, D. R. Ashok, and A. Chockalingam, “Joint NOMA transmission in indoor multi-cell VLC networks,” in *Proc. IEEE 30th Ann. Int. Symp. Pers., Indoor Mob. Radio Commun.*, Sep. 2019, pp. 1–6.

[77] J. Shi, J. He, K. Wu, and J. Ma, “Enhanced performance of asynchronous multi-cell VLC system using OQAM/OFDM-NOMA,” *J. Lightw. Technol.*, vol. 37, no. 20, pp. 5212–5220, Oct. 2019.

[78] A. Benjebbovu, A. Li, Y. Saito, Y. Kishiyama, A. Harada, and T. Nakamura, “System-level performance of downlink noma for future LTE enhancements,” in *Proc. IEEE Globecom Workshops*, 2013, pp. 66–70.

[79] M. A. Sedaghat and R. R. Müller, “On user pairing in uplink noma,” *IEEE Trans. Wireless Commun.*, vol. 17, no. 5, pp. 3474–3486, May 2018.

[80] Z. Q. Al-Abbasi and D. K. C. So, “User-pairing based non-orthogonal multiple access (NOMA) system,” in *Proc. IEEE 83rd Veh. Technol. Conf.*, 2016, pp. 1–5.

[81] L. Zhu, J. Zhang, Z. Xiao, X. Cao, and D. O. Wu, “Optimal user pairing for downlink non-orthogonal multiple access (NOMA),” *IEEE Wireless Commun. Lett.*, vol. 8, no. 2, pp. 328–331, Apr. 2019.

[82] J. He, Z. Tang, and Z. Che, “Fast and efficient user pairing and power allocation algorithm for non-orthogonal multiple access in cellular networks,” *IET Electron. Lett.*, vol. 52, no. 25, pp. 2065–2067, 2016.

[83] E. M. Almohimmah, M. T. Alresheedi, A. F. Abas, and J. Elmirghani, “A simple user grouping and pairing scheme for non-orthogonal multiple access in VLC system,” in *Proc. Int. Conf. Transp. Opt. Nets.*, Jul. 2018, pp. 1–4.

[84] Y. Yapici and I. Guvenc, “Non-orthogonal multiple access for mobile VLC networks with random receiver orientation,” in *Proc. IEEE Glob. Commun. Conf.*, Dec. 2019, pp. 1–6.

[85] H. Abumarshoud, H. Alshaer, and H. Haas, “Dynamic multiple access configuration in intelligent LiFi attocellular access points,” *IEEE Access*, vol. 7, pp. 62 126–62 141, May 2019.

[86] M. B. Janjua, D. B. da Costa, and H. Arslan, “User pairing and power allocation strategies for 3d VLC-NOMA systems,” *IEEE Wireless Commun. Lett.*, vol. 9, no. 6, pp. 866–870, Jun. 2020.

[87] V. K. Papanikolaou, P. D. Diamantoulakis, and G. K. Karagiannidis, “User grouping for hybrid VLC/RF networks with noma: A coalitional game approach,” *IEEE Access*, vol. 7, pp. 103 299–103 309, 2019.

[88] V. K. Papanikolaou, P. D. Diamantoulakis, Z. Ding, S. Muhaidat, and G. K. Karagiannidis, “Hybrid VLC/RF networks with non-orthogonal multiple access,” in *Proc. IEEE Global Commun. Conf.*, Dec. 2018, pp. 1–6.

[89] X. Zhou, S. Li, H. Zhang, Y. Wen, Y. Han, and D. Yuan, “Cooperative NOMA based VLC/RF system with simultaneous wireless information and power transfer,” in *Proc. IEEE/CIC Int. Conf. Commun. China*, Aug. 2018, pp. 100–105.

[90] M. K. A. Aljohani, M. O. I. Musa, M. T. Alresheedi, and J. M. H. Elmirghani, “WDM NOMA VLC systems,” in *Proc. 21st Int. Conf. Transp. Opt. Nets.*, Jul. 2019, pp. 1–5.

[91] Q. H. Spencer, C. B. Peel, A. L. Swindlehurst, and M. Haardt, “An introduction to the multi-user MIMO downlink,” *IEEE Commun. Mag.*, vol. 42, no. 10, pp. 60–67, Oct. 2004.

[92] Q. H. Spencer, A. L. Swindlehurst, and M. Haardt, “Zero-forcing methods for downlink spatial multiplexing in multiuser MIMO channels,” *IEEE Trans. Signal Process.*, vol. 52, no. 2, pp. 461–471, Feb. 2004.

[93] J. Chen, Y. Hong, Z. Wang, and C. Yu, “Precoded visible light communications,” in *Proc. 9th Int. Conf. Inf., Commun. Signal Process.*, Dec. 2013, pp. 1–4.

[94] Y. Hong, J. Chen, Z. Wang, and C. Yu, “Performance of a precoding MIMO system for decentralized multiuser indoor visible light communications,” *IEEE Photon. J.*, vol. 5, no. 4, pp. 7 800 211–7 800 211, Aug. 2013.

[95] Z. Yu, R. J. Baxley, and G. T. Zhou, “Multi-user MISO broadcasting for indoor visible light communication,” in *Proc. IEEE Int. Conf. Acoust., Speech Signal Process.*, May 2013, pp. 4849–4853.

[96] H. Ma, L. Lampe, and S. Hranilovic, “Robust MMSE linear precoding for visible light communication broadcasting systems,” in *Proc. IEEE Globecom Workshops*, Dec. 2013, pp. 1081–1086.

[97] B. Li, J. Wang, R. Zhang, H. Shen, C. Zhao, and L. Hanzo, “Multiuser MISO transceiver design for indoor downlink visible light communication under per-LED optical power constraints,” *IEEE Photon. J.*, vol. 7, no. 4, pp. 1–15, Aug. 2015.

[98] T. V. Pham, H. Le-Minh, and A. T. Pham, “Multi-user visible light communication broadcast channels with zero-forcing precoding,” *IEEE Trans. Commun.*, vol. 65, no. 6, pp. 2509–2521, Jun. 2017.

[99] H. Shen, Y. Deng, W. Xu, and C. Zhao, “Rate maximization for downlink multiuser visible light communications,” *IEEE Access*, vol. 4, pp. 6567–6573, Sep. 2016.

[100] H. Marshoud, P. C. Sofotasios, S. Muhaidat, B. S. Sharif, and G. K. Karagiannidis, “Optical adaptive precoding for visible light communications,” *IEEE Access*, vol. 6, pp. 22 121–22 130, Mar. 2018.

[101] Q. Wang, Z. Wang, and L. Dai, “Multiuser MIMO-OFDM for visible light communications,” *IEEE Photon. J.*, vol. 7, no. 6, pp. 1–11, Dec. 2015.

[102] Z. Zeng and H. Du, “Robust precoding scheme for multi-user MIMO visible light communication system,” in *Proc. 25th Europ. Signal Process. Conf.*, Aug. 2017, pp. 2546–2550.

[103] K. Ying, H. Qian, R. J. Baxley, and S. Yao, “Joint optimization of precoder and equalizer in MIMO VLC systems,” *IEEE J. Sel. Areas Commun.*, vol. 33, no. 9, pp. 1949–1958, Sep. 2015.

[104] P. Adasme, F. Seguel, I. Soto, and E. S. Juan, “Spatial time division multiple access for visible light communication networks,” in *Proc. 1st South Amer. Coll. Visible Light Commun.*, Nov. 2017, pp. 1–6.

[105] H. Ma, L. Lampe, and S. Hranilovic, “Coordinated broadcasting for multiuser indoor visible light communication systems,” *IEEE Trans. Commun.*, vol. 63, no. 9, pp. 3313–3324, Sep. 2015.

[106] H. Ma, A. Mostafa, L. Lampe, and S. Hranilovic, “Coordinated beamforming for downlink visible light communication networks,” *IEEE Trans. Commun.*, vol. 66, no. 8, pp. 3571–3582, Aug. 2018.

[107] L. Yin, X. Wu, and H. Haas, “SDMA grouping in coordinated multipoint VLC systems,” in *Proc. IEEE Summer Topic. Meet. Ser. (SUM)*, Jul. 2015, pp. 169–170.

[108] L. Yin, X. Wu, H. Haas, and L. Hanzo, “Low-complexity SDMA user-grouping for the CoMP-VLC downlink,” in *Proc. IEEE Global Commun. Conf.*, Dec. 2015, pp. 1–6.

[109] J. B. Carruther and J. M. Kahn, “Angle diversity for nondirected wireless infrared communication,” *IEEE Trans. Commun.*, vol. 48, no. 6, pp. 960–969, Jun. 2000.

[110] S.-M. Kim and H.-J. Lee, “Visible light communication based on space-division multiple access optical beamforming,” *Chin. Opt. Lett.*, vol. 12, no. 12, pp. 120 601–120 601, Dec. 2014.

[111] Z. Chen and H. Haas, “Space division multiple access in visible light communications,” in *Proc. IEEE Int. Conf. Commun.*, Jun. 2015, pp. 5115–5119.

[112] Z. Chen, D. A. Basnayaka, and H. Haas, “Space division multiple access for optical attocell network using angle diversity transmitters,” *J. Lightw. Technol.*, vol. 35, no. 11, pp. 2118–2131, Jun. 2017.

[113] G. Xu and S. Li, “Throughput multiplication of wireless LANs for multimedia services: SDMA protocol design,” in *Proc. IEEE Globecom Commun.*, vol. 3, Nov. 1994, pp. 1326–1332.

[114] H. Sifaou, A. Kammoun, K. Park, and M. Alouini, “Robust transceivers design for multi-stream multi-user MIMO visible light communication,” *IEEE Access*, vol. 5, pp. 26 387–26 399, Nov. 2017.

[115] Te Han and K. Kobayashi, “A new achievable rate region for the interference channel,” *IEEE Trans. Inf. Theory*, vol. 27, no. 1, pp. 49–60, Jan. 1981.

[116] B. Clerckx, H. Joudeh, C. Hao, M. Dai, and B. Rassouli, “Rate splitting for MIMO wireless networks: A promising PHY-layer strategy for LTE evolution,” *IEEE Commun. Mag.*, vol. 54, no. 5, pp. 98–105, May 2016.

[117] M. Dai, B. Clerckx, D. Gesbert, and G. Caire, “A rate splitting strategy for massive MIMO with imperfect CSIT,” *IEEE Trans. Wireless Commun.*, vol. 15, no. 7, pp. 4611–4624, Jul. 2016.

[118] M. Dai and B. Clerckx, “Multiuser millimeter wave beamforming strategies with quantized and statistical CSIT,” *IEEE Trans. Wireless Commun.*, vol. 16, no. 11, pp. 7025–7038, Nov. 2017.

[119] H. Joudeh and B. Clerckx, “Rate-splitting for max-min fair multigroup multicast beamforming in overloaded systems,” *IEEE Trans. Wireless Commun.*, vol. 16, no. 11, pp. 7276–7289, Nov. 2017.

[120] A. Papazafeiropoulos, B. Clerckx, and T. Ratnarajah, “Rate-splitting to mitigate residual transceiver hardware impairments in massive MIMO systems,” *IEEE Trans. Veh. Technol.*, vol. 66, no. 9, pp. 8196–8211, Sep. 2017.

[121] A. Salem, C. Masouros, and B. Clerckx, “Rate splitting with finite constellations: The benefits of interference exploitation vs suppression,” 2019, *arXiv:1907.08457*.

[122] Y. Mao and B. Clerckx, “Beyond dirty paper coding for multi-antenna broadcast channel with partial CSIT: A rate-splitting approach,” *IEEE Trans. Commun.*, vol. 68, no. 11, pp. 6775–6791, Nov. 2020.

[123] C. Hao, Y. Wu, and B. Clerckx, “Rate analysis of two-receiver miso broadcast channel with finite rate feedback: A rate-splitting approach,” *IEEE Trans. Commun.*, vol. 63, no. 9, pp. 3232–3246, Sep. 2015.

[124] G. Zhou, Y. Mao, and B. Clerckx, “Rate-splitting multiple access for multi-antenna downlink communication systems: Spectral and energy efficiency tradeoff,” 2020, *arVix:2001.03206*.

[125] Y. Mao, B. Clerckx, and V. O. K. Li, “Rate-splitting for multi-user multi-antenna wireless information and power transfer,” in *Proc. IEEE 20th Int. Workshop. Signal Process. Adv. Wireless Commun.*, Jul. 2019, pp. 1–5.

[126] Y. Mao, B. Clerckx, and V. O. K. Li, “Rate-splitting multiple access for coordinated multi-point joint transmission,” in *Proc. IEEE Int. Conf. Commun. Workshops.*, May 2019, pp. 1–6.

[127] J. Zhang, B. Clerckx, J. Ge, and Y. Mao, “Cooperative rate splitting for MISO broadcast channel with user relaying, and performance benefits over cooperative NOMA,” *IEEE Signal Process. Lett.*, vol. 26, no. 11, pp. 1678–1682, Nov. 2019.

[128] Y. Mao, B. Clerckx, J. Zhang, V. O. K. Li, and M. Arafah, “Max-min fairness of K-user cooperative rate-splitting in MISO broadcast channel with user relaying,” *IEEE Trans. Wireless Commun.*, vol. 19, no. 10, pp. 6362–6376, Oct. 2020.

[129] A. Papazafeiropoulos and T. Ratnarajah, “Rate-splitting robustness in multi-pair massive MIMO relay systems,” *IEEE Trans. Wireless Commun.*, vol. 17, no. 8, pp. 5623–5636, Aug. 2018.

[130] D. Yu, J. Kim, and S. Park, "An efficient rate-splitting multiple access scheme for the downlink of C-RAN systems," *IEEE Wireless Commun. Lett.*, vol. 8, no. 6, pp. 1555–1558, Dec. 2019.
[131] L. Yin and B. Clerckx, "Rate-splitting multiple access for multibeam satellite communications," *ArXiv*, vol. abs/2002.01731, 2020.
[132] A. Rahmati, Y. Yapici, N. Rupasinghe, I. Guvenc, H. Dai, and A. Bhuyan, "Energy efficiency of RSMA and NOMA in cellular-connected mmWave UAV networks," in *Proc. IEEE Int. Conf. Commun. Workshops.*, May 2019, pp. 1–6.
[133] G. Stepniak, J. Siuzdak, and P. Zwierko, "Compensation of a VLC phosphorescent white LED nonlinearity by means of Volterra DFE," *IEEE Photon. Technol. Lett.*, vol. 25, no. 16, pp. 1597–1600, Aug. 2013.
[134] D. H. Nguyen and T. Le-Ngoc, "MMSE precoding for multiuser MISO downlink transmission with non-homogeneous user SNR conditions," *EURASIP J. Adv. Signal Process.*, vol. 2014, no. 1, p. 85, Jun. 2014.
[135] S. S. Christensen, R. Agarwal, E. De Carvalho, and J. M. Cioffi, "Weighted sum-rate maximization using weighted MMSE for MIMO-BC beamforming design," *IEEE Trans. Wireless Commun.*, vol. 7, no. 12, pp. 4792–4799, Dec. 2008.
[136] M. Grant and B. SP, "CVX: MATLAB software for disciplined convex programming," Jan. 2014. [Online]. Available: http://cvxr.com/cvx/
[137] N. Raveendran, H. Zhang, D. Niyato, F. Yang, J. Song, and Z. Han, "VLC and D2D heterogeneous network optimization: A reinforcement learning approach based on equilibrium problems with equilibrium constraints," *IEEE Trans. Wireless Commun.*, vol. 18, no. 2, pp. 1115–1127, Feb. 2019.

**SHIMAA NASER** received the M.Sc. degree in electrical engineering from the Jordan University of Science and Technology, Irbid, Jordan, in 2015. Since 2018, she has been working toward the Ph.D. degree with the Department of Electrical and Computer Engineering, Khalifa University, Abu Dhabi, UAE. Her research interests include advanced digital signal processing and modulation techniques for visible light communications, MIMO-based communication, and orthogonal/non-orthogonal multiple access.

**PASCHALIS C. SOFOTASIOS** (Senior Member, IEEE) was born in Volos, Greece, in 1978. He received the M.Eng. degree from Newcastle University, Newcastle upon Tyne, U.K., in 2004, the M.Sc. degree from the University of Surrey, Guildford, U.K., in 2006, and the Ph.D. degree from the University of Leeds, Leeds, U.K., in 2011.

He has held academic positions with the University of Leeds, U.K., University of California at Los Angeles, CA, USA, Tampere University of Technology, Finland, Aristotle University of Thessaloniki, Greece, and Khalifa University of Science and Technology, UAE, where he currently serves as an Assistant Professor with the Department of Electrical Engineering and Computer Science. His M.Sc. studies were funded by a scholarship from UK-EPSRC and his Doctoral studies were sponsored by UK-EPSRC and Pace plc. His research interests are in the broad areas of digital and optical wireless communications as well as in topics relating to special functions and statistics.

Dr. Sofotasios serves as a regular Reviewer for several international journals and has been a TPC Member and TPC Chair of numerous IEEE conferences. He currently serves as an Editor for the IEEE COMMUNICATIONS LETTERS and he received the Exemplary Reviewer Award from the IEEE COMMUNICATIONS LETTERS in 2012 and the IEEE TRANSACTIONS ON COMMUNICATIONS in 2015 and 2016. He received the Best Paper Award at ICUFN 2013.

**LINA BARIAH** (Member, IEEE) received the M.Sc. and Ph.D. degrees in communications engineering from Khalifa University, Abu Dhabi, UAE, in 2015 and 2018, respectively. She is currently a Postdoctoral Fellow with the KU Center for Cyber-Physical Systems, Khalifa University. She was a Visiting Researcher with the Department of Systems and Computer Engineering, Carleton University, ON, Canada, in summer 2019. Her research interests include advanced digital signal processing techniques for communications, channel estimation, cooperative communications, non-orthogonal multiple access, cognitive radios, and intelligent surfaces.

**WAEL JAAFAR** (Senior Member, IEEE) received the B.Eng. degree from the Higher School of Communication (SUPCOM), Tunis, Tunisia, in 2007, and the M.A.Sc. and Ph.D. degrees in electrical engineering from Polytechnique Montreal, Montreal, QC, Canada, in 2009 and 2014, respectively. He was a Visiting Research Intern with the Department of Computer Science, UQAM, Montreal, Canada, between February 2007 and April 2007, and a Visiting Researcher with Keio University, Tokyo, Japan, between March 2013 and June 2013, and with Khalifa University, Abu Dhabi, UAE, between November and December 2019. From 2014 to 2017, he has pursued a career in the telecommunications industry, where he has been involved in designing solutions for projects across Canada and abroad. In 2018, he held Research Fellow and Lecturer positions with the Computer Science Department, UQAM, Montreal, Canada. Since December 2018, he joined the Systems and Computer Engineering Department, Carleton University as an NSERC (National Sciences and Engineering Research Council of Canada) Postdoctoral Fellow. His current research interests include wireless communications, aerial networks, resource allocation, edge caching and computing, and machine learning.

**SAMI MUHAIDAT** (Senior Member, IEEE) received the Ph.D. degree in electrical and computer engineering from the University of Waterloo, Waterloo, ON, Canada, in 2006.

From 2007 to 2008, he was an NSERC Postdoctoral Fellow with the Department of Electrical and Computer Engineering, University of Toronto, ON, Canada. From 2008 to 2012, he was an Assistant Professor with the School of Engineering Science, Simon Fraser University, Burnaby, BC, Canada. He is currently a Full Professor with Khalifa University, Abu Dhabi, UAE, an Adjunct Professor with the Department of Systems and Computer Engineering, Carleton University, Ottawa, ON, Canada, and a Visiting Reader with the Faculty of Engineering, University of Surrey, Guildford, U.K.

Dr. Muhaidat currently serves as an Area Editor for the IEEE TRANSACTIONS ON COMMUNICATIONS, and he was previously a Senior Editor for the IEEE COMMUNICATIONS LETTERS and an Associate Editor for the IEEE TRANSACTIONS ON COMMUNICATIONS, IEEE COMMUNICATIONS LETTERS, and IEEE TRANSACTIONS ON VEHICULAR TECHNOLOGY. He was the recipient of several scholarships during his undergraduate and graduate studies and the winner of the 2006 NSERC Postdoctoral Fellowship Competition.

**MAHMOUD AL-QUTAYRI** (Senior Member, IEEE) received the B.Eng. degree from Concordia University, Montreal, QC, Canada, in 1984, the M.Sc. degree from the University of Manchester, Manchester, U.K., in 1987, and the Ph.D. degree from the University of Bath, Bath, U.K., in 1992, all in electrical and electronic engineering. He is currently the Associate Dean for Graduate Studies - College of Engineering, and a Professor of electrical and computer engineering with Khalifa University, Abu Dhabi, UAE. Prior to joining Khalifa University, he was a Senior Lecturer with De Montfort University, U.K. This was preceded by a Research Officer appointment with the University of Bath. He has published numerous technical papers in peer reviewed international journals and conferences and he has coauthored a book as well as a number of book chapters. His main fields of research include embedded systems design, applications and security, design and test of mixed-signal integrated circuits, wireless sensor networks, and cognitive wireless networks. During his academic career, he made many significant contributions to both undergraduate as well as graduate education. His professional service includes membership of the steering, organizing and technical program committees of many international conferences.

**OCTAVIA A. DOBRE** (Fellow, IEEE) received the Dipl.Ing. and Ph.D. degrees from Politehnica University of Bucharest (formerly Polytechnic Institute of Bucharest), Bucharest, Romania, in 1991 and 2000, respectively.

Between 2002 and 2005, she was with the New Jersey Institute of Technology, USA and Politehnica University of Bucharest. In 2005, she joined Memorial University, John's, NL, Canada, where she is currently a Professor and Research Chair. She was a Visiting Professor with the Massachusetts Institute of Technology, USA and Université de Bretagne Occidentale, France. Her research interests include enabling technologies for beyond 5G, blind signal identification and parameter estimation techniques, as well as optical and underwater communications. She has authored or coauthored more than 300 refereed papers in these areas.

Dr. Dobre serves as the Editor-in-Chief (EiC) of the IEEE Open Journal of the Communications Society and an Editor for the IEEE COMMUNICATIONS SURVEYS AND TUTORIALS. She was the EiC for the IEEE COMMUNICATIONS LETTERS, as well as a Senior Editor, an Editor, and a Guest Editor for various prestigious journals and magazines. She was the General Chair, Technical Program Co-Chair, Tutorial Co-Chair, and Technical Co-Chair of symposia at numerous conferences. She was a Royal Society Scholar and a Fulbright Scholar. She obtained Best Paper Awards at various conferences, including IEEE ICC, IEEE Globecom, IEEE WCNC, and IEEE PIMRC. She is a Distinguished Lecturer of the IEEE Communications Society and a Fellow of the Engineering Institute of Canada.